Progress in Oceanography 176 (2019) 102139

Contents lists available at ScienceDirect

Progress in Oceanography

journal homepage: www.elsevier.com/locate/pocean

Revisiting the circulation of the East Australian Current: Its path, separation, and eddy field

Peter R. Oke[a,*], Moninya Roughan[b], Paulina Cetina-Heredia[b], Gabriela S. Pilo[a,c], Kenneth R. Ridgway[a], Tatiana Rykova[a], Matthew R. Archer[b], Richard C. Coleman[c], Colette G. Kerry[b], Carlos Rocha[b], Amandine Schaeffer[b], Eduardo Vitarelli[b]

[a] CSIRO Oceans and Atmosphere, Hobart, TAS, Australia
[b] School of Mathematics and Statistics, University of New South Wales, Sydney, NSW, Australia
[c] University of Tasmania, Hobart, TAS, Australia

ARTICLE INFO

Keywords:
East Australian Current
Ocean circulation
Ocean eddies
Western boundary currents

ABSTRACT

The traditional view of the East Australian Current (EAC), as depicted in many schematics, is of a continuous boundary current that flows along the shelf off eastern Australia, between approximately 18°S and about 32.5°S, where it separates from the coast and continues either towards New Zealand, along the Tasman Front; or towards Tasmania, as the EAC Extension. Additionally, it is widely recognised that eddies are prevalent in the EAC region – particularly south of the EAC separation. We revisit this long-standing paradigm and suggest that the EAC is perhaps better viewed as a continuous, meandering stream, flowing adjacent to the coast that "feeds" a field of mesoscale eddies. Observations show that EAC eddies are prevalent over a broad region of the western Tasman Sea, as far north as 25°S, typically with maximum intensity between 30 and 35°S. At any instant in time the EAC jet is usually evident as a poleward stream adjacent to the continental shelf edge. Other commonly accepted components of the EAC System, including the Tasman Front and EAC Extension, are rarely seen as distinct, identifiable features. Rather, these features are evident only in time-mean fields, when the eddy-variability is filtered out. It is also common for the EAC to be spatially discontinuous – due to the presence of eddies – often with multiple short streams that sometimes separate and re-attach to the coast. Recognition of the EAC as an eddy-dominated current system has seen many recent studies focus on various aspects of eddies in the EAC System, providing new insights into mesoscale ocean dynamics. Recent studies of individual eddies have shown that the circulation within eddies, including tilting and vertical motion, is more complex than previously understood. A summary of these studies, along with a review of the EAC System, particularly its path, separation, and eddy field is presented here.

1. Introduction

The East Australian Current (EAC) is the Western Boundary Current (WBC) of the sub-tropical Pacific Ocean. The EAC is important for its role in the transport of heat, marine biota, and debris, and for its influence on primary production, weather, and climate. In this paper, we challenge the traditional view of the East Australian Current (EAC) by asking whether the "Tasman Front" (e.g., Denham and Crook, 1976; Stanton, 1979; Andrews et al., 1980; Stanton, 1981; Mata et al., 2006; Sutton and Bowen, 2014; Oke et al. 2019) really exists; and questioning whether a continuous "EAC Extension" (e.g., Godfrey et al., 1980; Speich et al., 2002; Ridgway and Dunn, 2003; van Sebille et al., 2012; Hill et al., 2011; Ganachaud et al., 2014; Ypma et al., 2016) can ever really be identified. These features of the EAC System are depicted in many published schematics (Fig. 1) – but are they present in observations of the ocean? There is broad acknowledgement of a complex field of EAC eddies post-separation (e.g., Godfrey et al., 1980; Bowen et al., 2005; Suthers et al., 2011; Everett et al., 2012) – but its not clear that the community has comprehensively answered the question posed by Hamon (1980), "The East Australian Current – continuous, or a series of eddies?" The original studies that first described these features in the 1970's and 80's were based on limited data – hypothesising about the presence and prevalence of these elements of the EAC System. Using the benefit of decades of observations, well-developed theories of ocean circulation, and mature, high-resolution models, we revisit these important elements of the EAC.

* Corresponding author.
E-mail address: Peter.oke@csiro.au (P.R. Oke).

https://doi.org/10.1016/j.pocean.2019.102139
Received 7 June 2018; Received in revised form 2 November 2018; Accepted 23 July 2019
Available online 24 July 2019

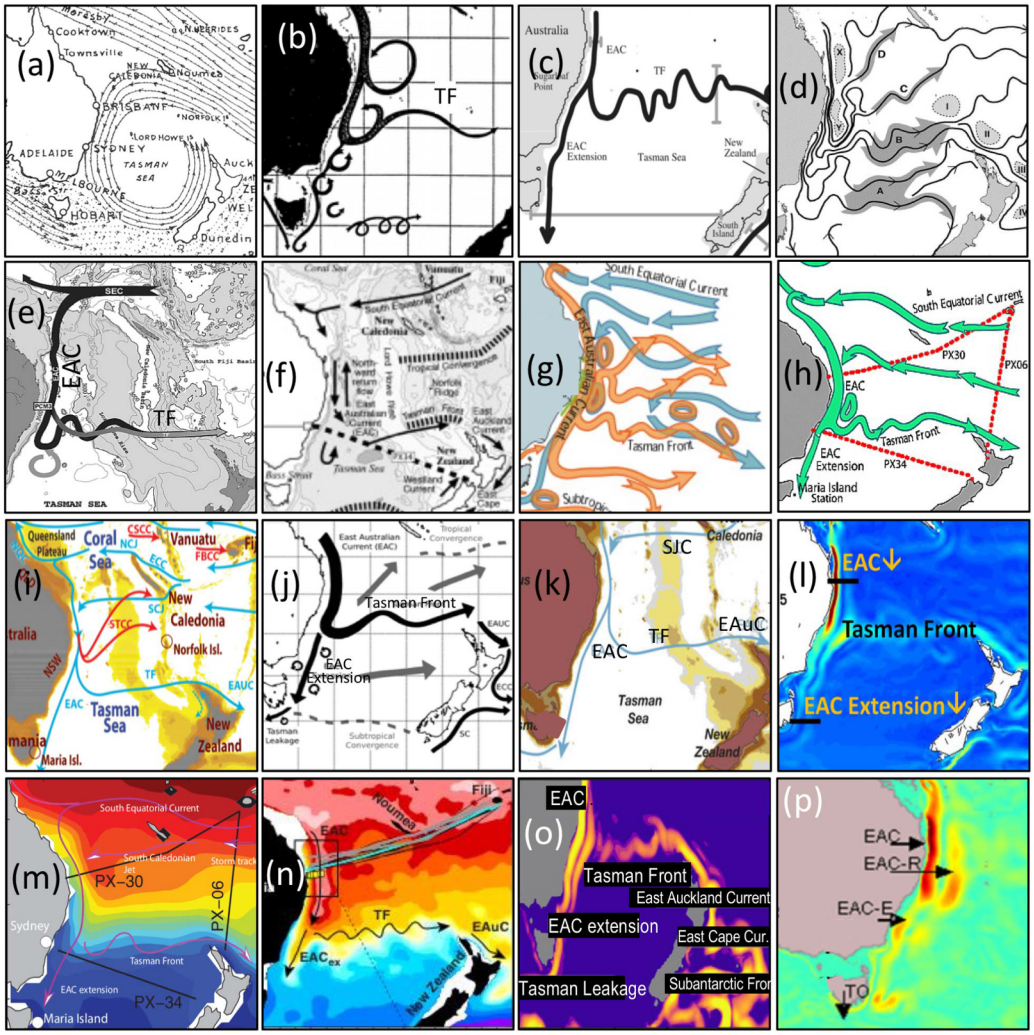

Fig. 1. Schematic representations of the ocean circulation off Eastern Australia, as depicted in various publications. Panels are presented in chronological order, and adapted from (a) Halligan (1921) (which was adapted from Black, 1853), (b) Church and Craig (1998),Tilburg et al. (2001), (d) Ridgway and Dunn (2003) and Mata et al. (2006), (f) Holbrook et al. (2011) and Condie et al. (2011), (h) (Hill et al., 2011), (i) Ganachaud et al. (2014) and Oliver and Holbrook (2014), (k) Hu et al. (2015) and Feng et al. (2016), (m) Sloyan et al. (2016) and Zilberman et al. (2018), (o) Bull et al. (2018), and (p) Wijeratne et al. (2018). Many of the schematics presented here include acronyms for specific elements. These are not all defined here, but the important ones are the EAC; EAC retroflection or return-flow (EAC-R in (p)); Tasman Front (TF in b, e, and n); the EAC Extension (EAC$_{EX}$ in n, EAC-E in p); and the Tasman Outflow (TO in p; equivalent to the Tasman Leakage in o).

In this paper, we conclude that the EAC is best described as a continuous current along the shelf that feeds a field of offshore eddies. Specifically, we suggest that the EAC is a continuous, meandering, poleward flow while it's "attached" to the shelf – that supplies energy to the field of offshore eddies after it separates from the coast (Fig. 2). This view of the EAC System is consistent with the insightful inference by Wyrtki (1962) and Godfrey et al. (1980), from just a few synoptic pictures of the system. We support this view throughout the paper, with references to recent and historical studies. The schematic in Fig. 2 depicts the permanent currents, the transient currents, and the eddy-components of the EAC System. The permanent currents include the branches of the South Equatorial Current (SEC), the EAC jet, and the East AUckland Current (EAUC). The transient currents include the EAC return flow, the flow between Australia and New Zealand – that Oke et al. 2019 refer to as the eastern extension of the (EAC); and the flow around Tasmania – that Oke et al. 2019 refer to as the southern extension of the EAC. The flow towards New Zealand is often depicted schematically as a permanent feature and is typically labelled the Tasman Front (Fig. 1). The flow adjacent to the coast towards Tasmania and the flow around Tasmania are also often represented as a permanent currents and are labelled the EAC Extension, Tasman Outflow, or Tasman Leakage (Fig. 1). The northward flow, offshore of the EAC jet, is often excluded from schematics (e.g., Fig. 1) but when it is included, it's typically implied to be permanent (Fig. 1). In this review, we show that these features are better considered as transient currents – and perhaps even as trains of eddies. This is represented more clearly in Fig. 2. The intent of including the example schematics in Fig. 1 is not to suggest that they are all wrong. In fact, we show that in a mean sense – most of the features represented are correct – but we think that the transient nature of the above-mentioned features is important, and needs explicit acknowledgement. Evidence for this refined picture of the EAC System is presented throughout this paper.

At any instant in time, the EAC region is often dominated by eddies, with a coherent boundary current only evident near the continental shelf. To demonstrate this, we present a series of snapshots of the EAC circulation, using satellite-derived fields for the first day of every month of 2016 (Fig. 3). In this series of images, the EAC is evident adjacent to the coast as a continuous stream, flowing southward between about 20°S and about 32–38°S. By contrast, the appearance of a coherent extension of the EAC away from the coast – either along the Tasman Front, or as the EAC Extension – is unclear (November is perhaps the only exception, where a coherent jet extends towards the centre of the Tasman Sea). In some cases, a northward-flowing return flow is evident (e.g., Feb, Jun). What seems more common, is for the EAC to break into multiple streams (e.g., Jul, Sep, Dec) and to become lost in a field of eddies (e.g., Feb, Mar, Apr, May). Every image in Fig. 3 includes multiple eddies that are present for all latitudes shown. This picture contrasts with other WBCs (see Fig. 4), where a long, continuous stream is often present. For the EAC, we observe that at no point in time is there evidence of a continuous, coherent flow along either the Tasman Front (Andrews et al., 1980), towards New Zealand; or the Tasman Outflow/Leakage, around Tasmania (Ridgway and Dunn, 2003). Rather, these features only become clear in time-averaged fields, as demonstrated in Fig. 5, showing examples of 1-year, 5-year, and 20-year averaged

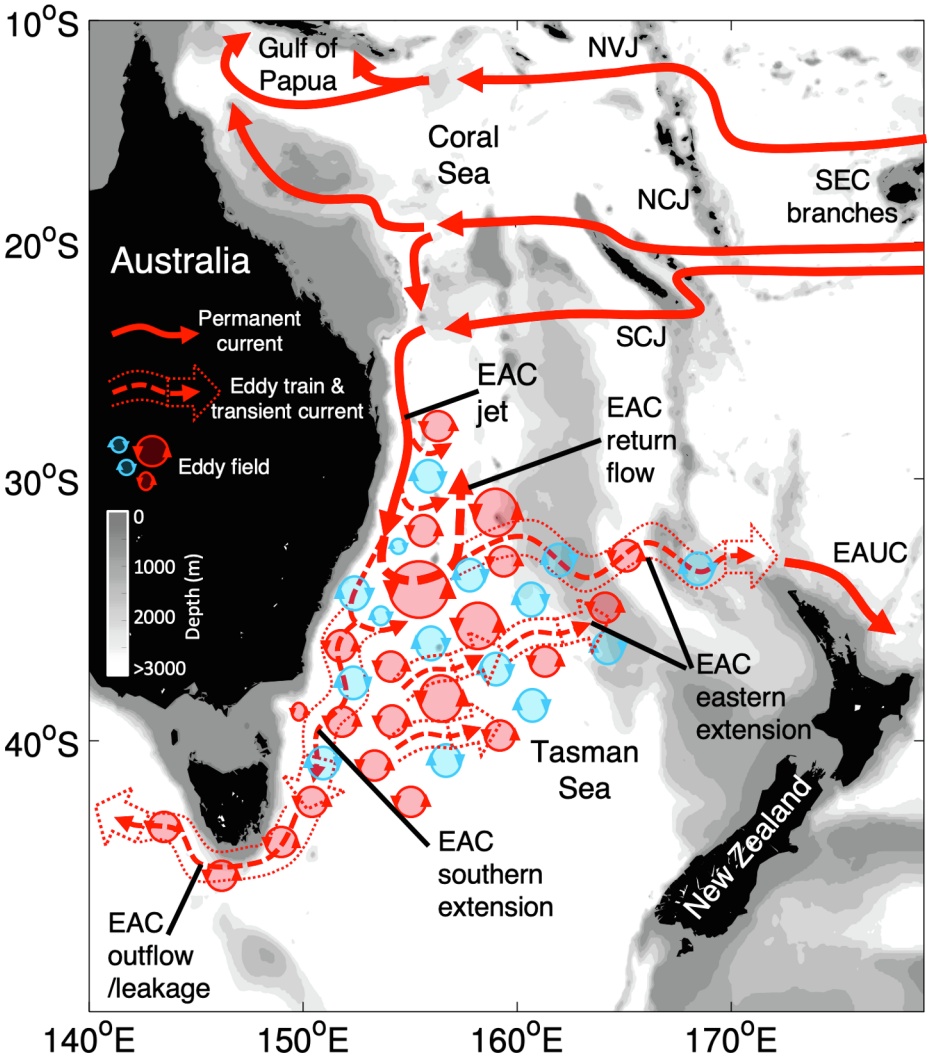

Fig. 2. Schematic showing the shallow (top ~1000 m) circulation of the EAC-portion of the South-Western Pacific Ocean. Red solid lines denote permanent currents; red dashed lines denote transient currents; the red bars denote "eddy trains"; and the red and blue circles denote the eddy field. EAUC = East Auckland Current; SEC = South Equatorial Current – depicted as three distinct branches; NVJ = North Vanuatu Jet; NCJ = North Caledonia Jet; SCJ = South Caledonia Jet; EAC = East Australian Current. (For interpretation of the references to colour in this figure legend, the reader is referred to the web version of this article.)

surface currents, derived from satellite data. This has been earlier demonstrated by Ridgway et al. (2008), showing that 10-day and 6-month averaged fields of EAC transport along the PX34 line (between Sydney and Auckland) were a discontinuous field of mesoscale eddies – and only after averaging did the picture of a continuous EAC jet prevail (Fig. 6).

Analysis of the EAC and its eddy field has undergone a continual transition. Early studies, in the 1970s and 1980s, focussed on the analysis of individual eddies (e.g., Boland and Hamon, 1970; Andrews and Scully-Power, 1976; Nilsson and Cresswell, 1980; Boland and Church, 1981; Tranter et al., 1982; Cresswell, 1983; Cresswell and Legeckis, 1986; Mulhearn et al., 1988). These studies showed remarkable insights – identifying eddy stacking, seasonal changes, and eddy merging events. Since those early studies, the availability of high-resolution satellite data, measuring sea-surface temperature and sea-level (e.g., Fig. 6) – as well as the emergence of large-scale eddy-resolving models (e.g., Fig. 4) and better quality in situ observations with greater spatial coverage – led many studies to examine the more general variability of the eddy field (e.g., statistical properties of the variability). This included the publication of a number of global "eddy databases" (e.g., Chelton et al., 2007; Chelton et al., 2011), permitting studies of the more general eddy characteristics for the first time (e.g., Everett et al., 2012; Pilo et al., 2015a). Over the last 10 years, there has been a tendency for the broad-scale analysis of eddies, including analyses of changes in circulation and properties in the Tasman Sea in climate downscaling studies (Chamberlain et al., 2012; Sun et al., 2012), to be complemented by analyses of individual eddies (e.g., Oke and Griffin, 2011; Baird et al., 2011; Macdonald et al., 2013, 2016; Pilo et al., 2015b; Roughan et al., 2017; Pilo et al., 2018), giving new insights into the details of eddy characteristics. We note that of the various studies cited above, the definition for the term "eddy" differs. For studies of individual eddies, an "eddy" tends to be regarded as an isolated, coherent vortex; and studies of eddy properties often attribute all signals that represent a departure from the mean state, as eddy variability (using the standard Reynolds decomposition). Many recent studies are reviewed in this manuscript, along with commentary, relating them to earlier works.

The most recent overview papers describing the EAC include the introduction to a special issue of *Continental Shelf Research*, by Suthers et al. (2011), and the SPICE (South Pacific Ocean Circulation and Climate Experiment; www.clivar.org/clivar-panels/pacific/spice) review by Ganachaud et al. (2014). Suthers et al. (2011) cited EAC-related papers covering topics that include circulation, biogeochemistry, and fisheries. Ganachaud et al. (2014) described the EAC with reference to

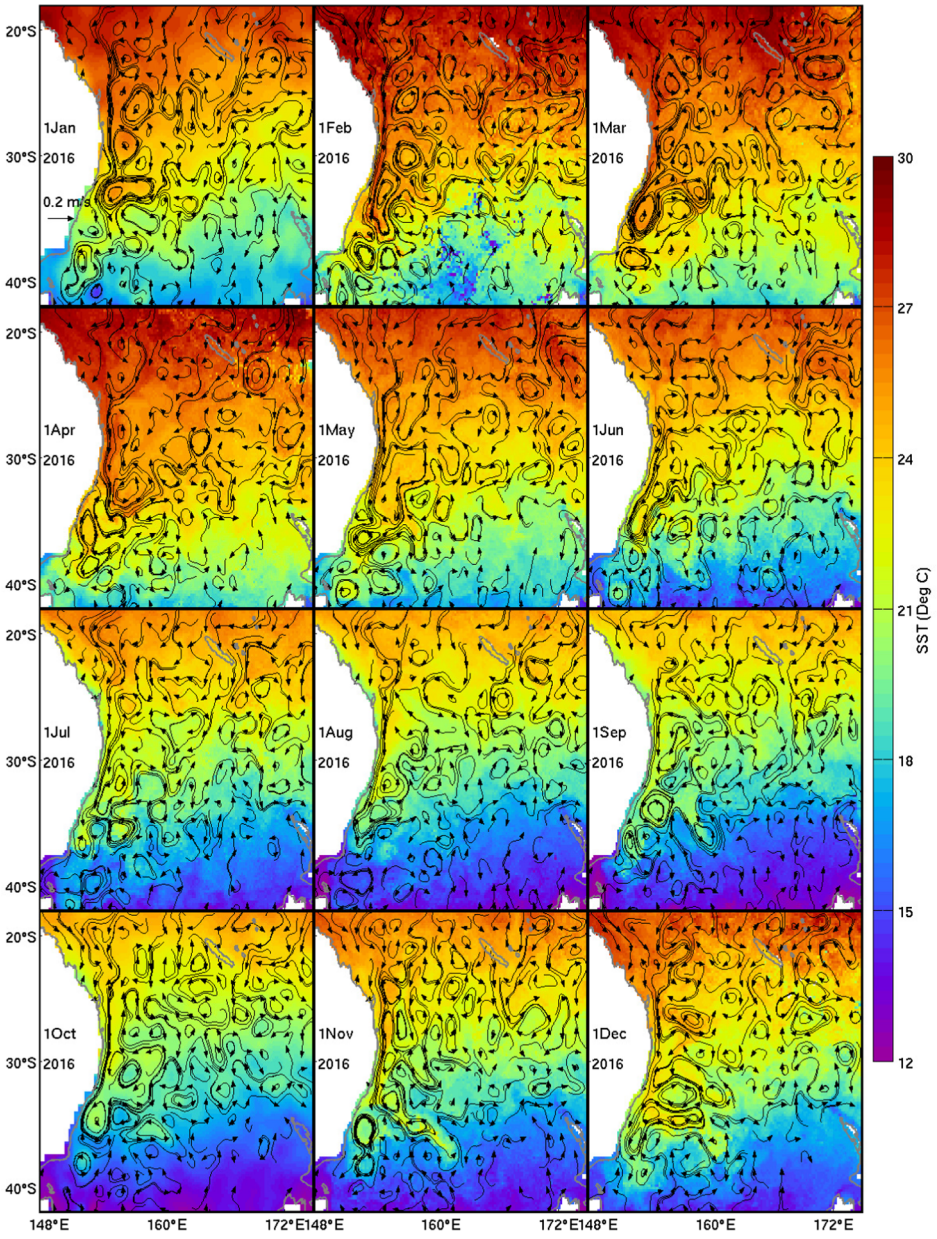

Fig. 3. Sample of synoptic snapshots of the circulation in the EAC region, using the 1st of each month for 2016, showing satellite SST (colour) and altimetry-derived surface geostrophic velocities (vectors). Fields are from OceanCurrent analyses (oceancurrent.imos.org.au) and show only vectors where the speed exceeds 0.1 m/s. The scale for velocity is shown in the top left panel.

the circulation in the Coral Sea. In this review paper, we limit our scope to the EAC System: including its path, separation, and eddy field. We here regard the EAC System to be approximately bounded by 18°S to the north, 45°S to the south, and extends between the Australian continent and about 180°E.

Throughout this paper we refer to separate, but related, aspects of the EAC System – namely the EAC jet, and the EAC eddy field. We refer to the EAC jet as the part of the EAC System that is characterised by a continuous, poleward-flowing current – typically "attached" to the coast. This definition highlights one of the key differences between the EAC and other WBCs, namely that the EAC jet doesn't usually extend offshore. Rather, the EAC tends to degenerate into an eddy train (Fig. 2); while the Gulf Stream and Kuroshio, for example, tend to continue offshore as meandering, inertial jets. By contrast to the EAC jet, we refer to the EAC eddy field as the complex field of eddies that is most prevalent in the western Tasman Sea. Based on this understanding of the different EAC System components, we organise this paper as follows. We describe historical and recent findings relating to the EAC jet in Section 2; the EAC separation in Section 3; the EAC eddy field in Section 4; an overview of studies of individual eddies in Section 5; and a description of recent studies on the interannual and decadal variability of the EAC in Section 6. We conclude in Section 7, including a description of knowledge gaps.

2. The EAC Jet

The EAC is the WBC of the South Pacific Ocean (Ridgway and Dunn, 2003), characterised by strong currents (typically 1 m/s) adjacent to the continental shelf, carrying warm (up to 22–26 °C) and salty (35–35.5 psu) waters southwards. The westward flow of the subtropical gyre, the South Equatorial Current, separates into a series of jets in the western Pacific Ocean, providing the source waters for the EAC (Ganachaud et al., 2014). The strongest of these westward jets is the southern branch of the North Caledonian Jet, "feeding" the EAC at

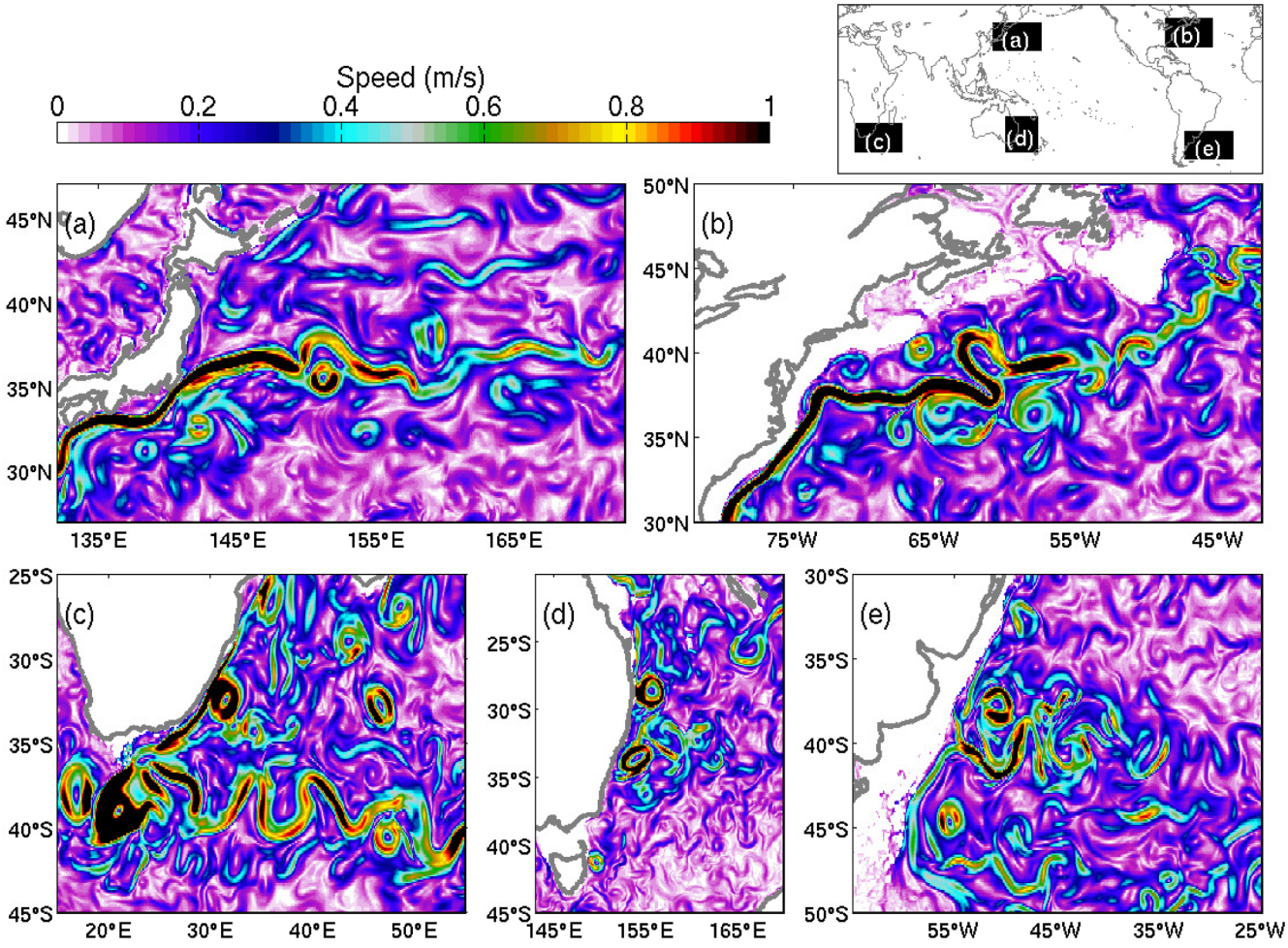

Fig. 4. Example of the circulation in the five main WBCs, namely the (a) Kuroshio Current, (b) Gulf Stream, (c) Agulhas Current, (d) EAC, and the Brazil-Malvinas Confluence, showing the current speed at 100 m depth in Ocean Forecast Australia Model (Oke et al., 2013) on 1 February 2009. The extent of each region is indicated in the top right panel.

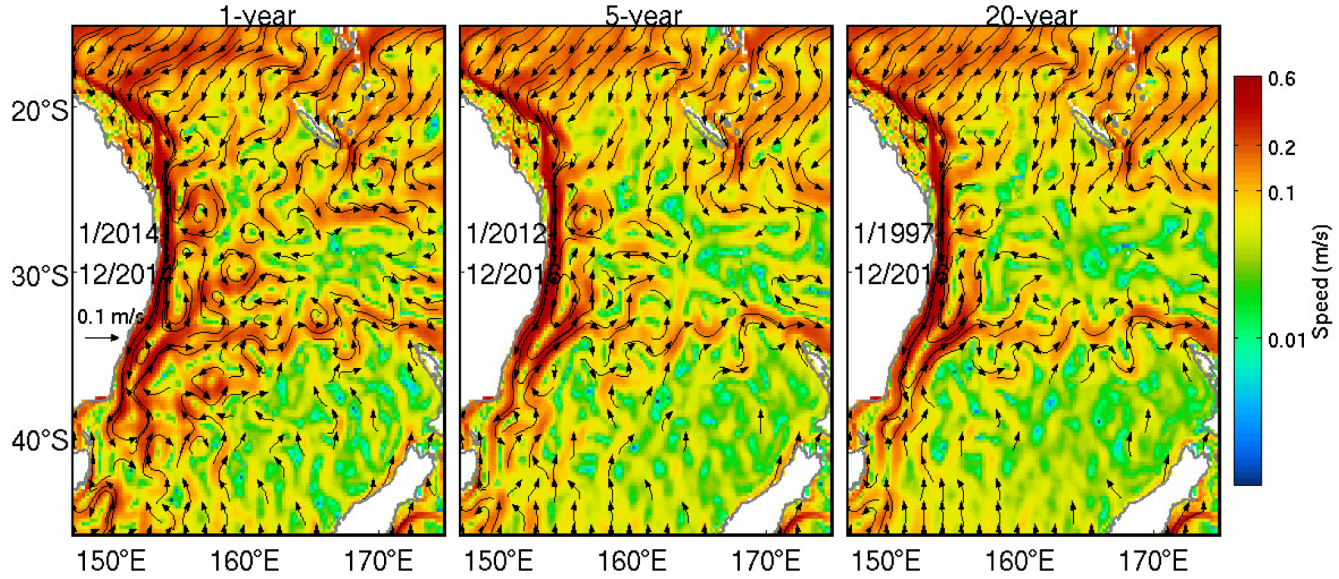

Fig. 5. Time-mean fields of surface geostrophic currents, plotted on a log-scale, from OceanCurrent, for a 1-year (2014; left), 5-year (2012–2016; middle), and 20-year (1997–2016; right) average. Colour shows the speed, and vectors are only shown in regions where the speed exceeds 0.05 m/s. (For interpretation of the references to colour in this figure legend, the reader is referred to the web version of this article.)

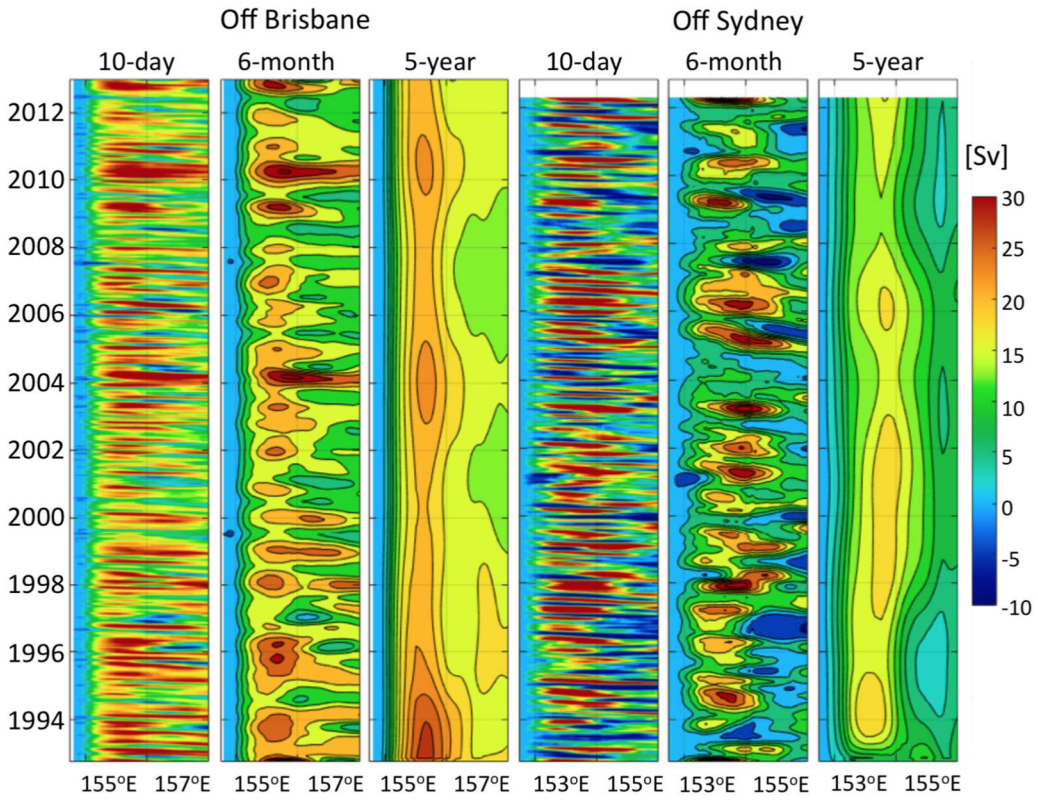

Fig. 6. The volume transport (relative to 2000 m; in Sv) off Brisbane (3 left panels) and Sydney (3 right panels) at the indicated timescales. The 10-day time series are generated using both XBT transects and altimetry (Ridgway et al., 2008).

approximately 18°S, and the South Caledonian Jet, entering the EAC System at about 22°S (Kessler and Cravatte, 2013). In this long-term average picture, the EAC is attached to the western boundary from its origin (around 18°S) until about 32°S, where a portion turns eastward, forming the Tasman Front (Denham and Crook, 1976; Stanton, 1979; Andrews et al., 1980), and a portion continues to flow along the boundary, as the EAC Extension (Godfrey et al., 1980). The mean eastward flow, that's typically referred to as the Tasman Front, is the connection to the subtropical gyre of the South Pacific Ocean (Reid, 1986); and the mean southward flow that's typically referred to as the EAC Extension is the connection to the super gyre – linking the three gyres of the Southern Hemisphere (Cai, 2006; Ridgway and Dunn, 2007). Analysis of the low-frequency circulation shows a "gating" between the flow along the "Tasman Front" and the flow along the "EAC Extension" (Hill et al., 2011) so that high-volume flow towards New Zealand corresponds to low-volume flow around Tasmania – and vice versa. There is evidence in modelling studies, with and without data assimilation (e.g., Koehl et al., 2007; Carton and Giese, 2008; Oke et al., 2008), that this gating has a quasi-decadal signal (Hill et al., 2011). Noting the absence of a meridional front across the Tasman Sea, Oke et al. (2019) suggest that the flow towards New Zealand should be referred to as the eastern extension of the EAC, and the flow towards Tasmania should be referred to as the southern extension of the EAC.

The typical picture of the EAC jet, described above, is represented schematically in Fig. 2 – including both "permanent" and "transient" currents. Only in time-averaged fields of sea-level and surface geostrophic currents (derived from altimetry), does clear evidence of a continuous flow towards New Zealand and around Tasmania emerge. In Fig. 2, we refer to this as an eddy train and transient current – as distinct from a continuous, meandering current (like those in the Gulf Stream and Kuroshio systems, for example). This is demonstrated in Fig. 3–6. Fig. 3 and 4 are described in Section 1, showing synoptic examples of the circulation in the EAC region. Fig. 5 shows fields of geostrophic velocity from a 1-year, 5-year, and 20-year averages. Even in time-mean fields in Fig. 5, the clear presence of a spatially-continuous flow along the paths referred to as the Tasman Front and EAC Extensions is not easily detected. The path of the Tasman Front in the time-means follows the path described previously (Tilburg et al., 2001; Ridgway and Dunn, 2003) that Ridgway and Dunn (2003) linked to topography.

The continuity (or lack of continuity) of the EAC jet in time is highlighted by the comparison of volume transports, computed from observations in Fig. 6. Fig. 6 shows Hovmoller diagrams of the volume transport (relative to 2000 m) off Brisbane and Sydney – constructed from a combination of temperature measurements from eXpendable BathyThermograph (XBT) transects and satellite altimetry (see Ridgway et al., 2008, for details) for 10-day averaged, 6-month averaged, and 5-year averaged time series for a 20-year period. In this comparison, the 10-day averaged time series shows high variability. Off Brisbane, the 10-day averaged transport varies significantly – but is mostly southward. This indicates that the EAC jet is always present as a coherent boundary current off Brisbane – but that its volume fluctuates as it meanders. By contrast, off Sydney, the 10-day averaged transport regularly fluctuates between positive (southward) and negative (northward). We interpret this as evidence of an eddy-dominated environment, with no clear boundary current off Sydney that is continuous in time (i.e., ever-present). By contrast, the 6-month averaged transport shows a southward-dominated (denoted by positive volume transport) current that is almost continuous in time, with periods of more/less intense flow. The 5-year averaged transport, both off Brisbane and Sydney, clearly shows a southward boundary current that is continuous in time.

Another way to understand the EAC circulation is by analysing the Lagrangian characteristics of the EAC – to determine how often Lagrangian particles follow the pathways associated with the Tasman Front, the EAC Extension, the EAC return flow, or EAC eddies. To

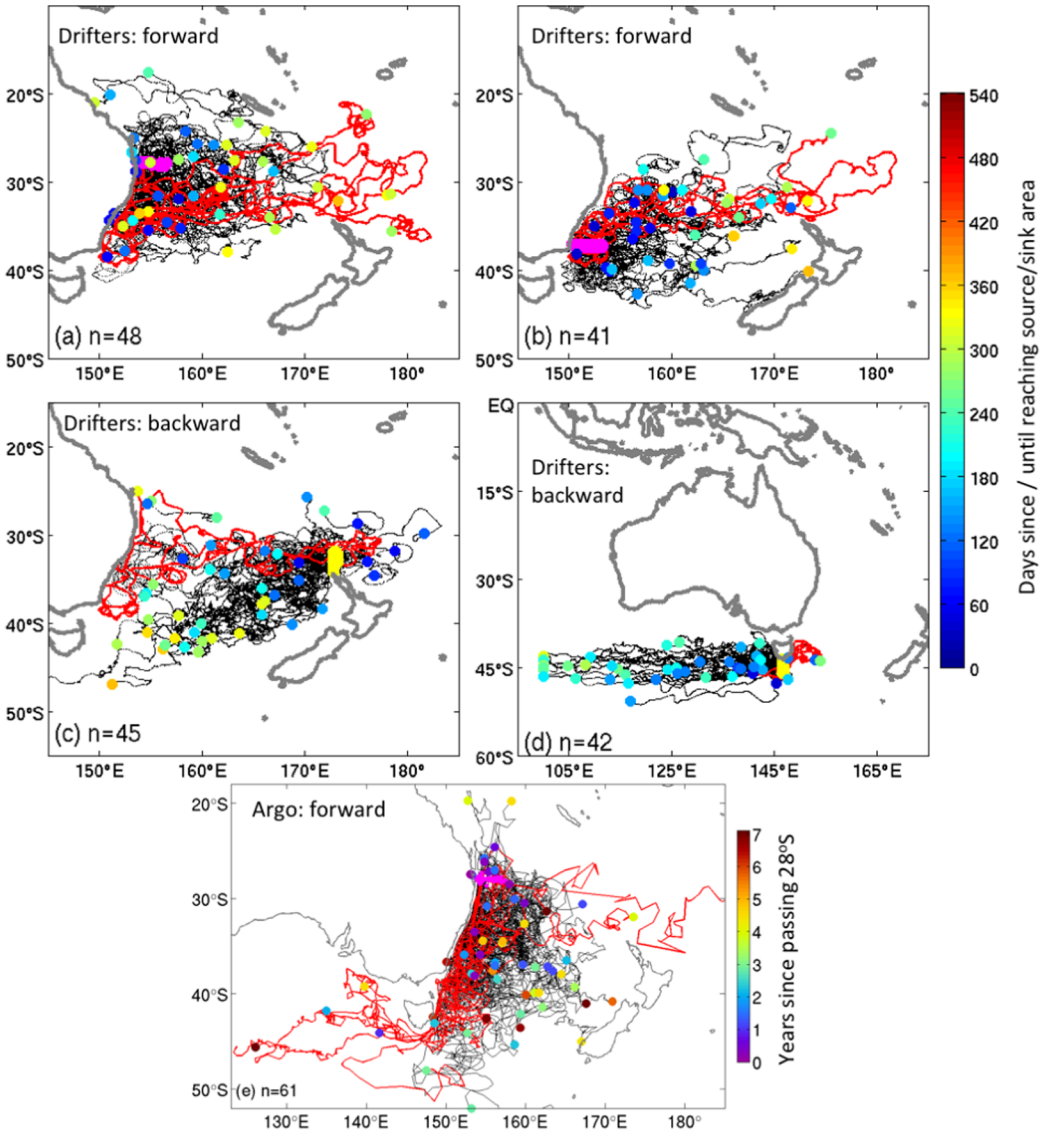

Fig. 7. Trajectories of (a–d) surface drifting buoys and (e) Argo floats that passed through different source/sink areas, denoted by the magenta/yellow dots, tracked forwards in time from within 300 km of the coast at (a, e) 28°S; and (b) 38°S; and tracked backwards in time from within 300 km of (c) the northern tip of New Zealand and (d) the southern tip of Tasmania. Trajectories are shown in black or red (red denotes trajectories that may have followed the path of either the EAC Extension or the Tasman Front); *n* denotes the number of drifters/floats. Coloured dots in panels a,b,e (panels c,d) denote the initial (final) location of each drifter/float, with the colour indicating the time until (since) the drifter/float entered the source area. Analysis uses 6-hourly drifter locations for 1993–2017 using drogued (at 15 m depth) and undrogued drifters; and 10-day Argo locations for 2001–2017 for floats with park depths of 1000 m. Data are sourced from AOML and the Argo GDAC. (For interpretation of the references to colour in this figure legend, the reader is referred to the web version of this article.)

achieve this, we analyse the path of all surface drifting buoys and Argo floats that passed through different geographic source/sink areas in the EAC region (Fig. 7). The drifters used here include both drogued (at 15 m depth) and undrogued drifters; and the Argo floats with a park depth of 1000 m, and including floats with both Iridium communications (that spend as little as 15 min at the surface every 10 days) and floats with Argos communications (that spend between 12 and 24 h at the surface every 10 days). Neither platform is a perfect Lagrangian particle for the circulation at the surface or 1000 m depth. The surface drifting buoys are subject to windage; and the Argo floats spend some time profiling through the water column (between the surface and 2000 m depth) and some time transmitting data to satellite at the surface. Another limitation of this analysis related to the lifetime of the instruments. The Argo floats typically operate for 4–5 years or more, which seems sufficient for a float to transit any of the paths of interest – but the surface drifting buoys are only designed to operate for 18 months. It's possible that drifters may reach end-of-life before fully transiting the pathways of interest. For this reason, we look at drifter trajectories starting in, or near, the EAC jet (Fig. 7a,b); and drifter trajectories ending in the choke points north of the northern tip of New Zealand (Fig. 7c) and south of Tasmania (Fig. 7d). For Argo floats, we only look at floats starting near the EAC jet (Fig. 7e). An alternative way to analyse Lagrangian paths of the EAC System is to use model results (e.g., van Sebille et al., 2012; Cetina-Heredia et al., 2015; Pilo et al., 2015b; Cetina-Heredia et al., 2019a. However, we have chosen to only use observations here, because some (probably all) models suffer from systematic errors that may be misleading (e.g., Oke et al., 2013).

The results in Fig. 7 provide limited support for the prevalence of the EAC Extension – with only 2–3 surface drifters (see Fig. 7d) and 4–5 Argo floats (see Fig. 7e), originating in the Tasman Sea, passing south of Tasmania. There is perhaps more evidence for flow along the path associated with the Tasman Front – with possibly up to 10 surface drifters passing the northern tip of New Zealand originating in the EAC jet (Fig. 7c implies at least 3; Fig. 7a,b implies 4–5). We also find that only one or two Argo floats, originating in the EAC jet, pass north of New Zealand (Fig. 7e), but this result is less meaningful because, with most Argo floats "parked" at 1000 m depth, the Lord Howe Rise obstructs the westward-advection of these floats across the Tasman Sea. Overwhelmingly, the trajectories presented in Fig. 7 indicate that most drifters/floats encountering the EAC jet end up trapped in the EAC eddy field – drifting either through the central Tasman Sea, towards New Zealand, until they reach end of life; or drifting around Tasmania, within eddies. Surface drifting buoys, trapped in the EAC eddy field, tend to drift eastwards, towards New Zealand – perhaps "weaving"

between eddies. We suggest that this eastward flow towards New Zealand "feeds" the inflow of the East Auckland Current (at the northern tip of New Zealand). Warren and Voorhis (1970) note that flow between the EAC and New Zealand, by some path, is necessary to satisfy the Sverdrup balance and the Island Rule (Godfrey, 1989; Risien and Chelton, 2008; Godfrey and Dunn, 2010; Colin de Verdière and Ollitrault, 2016). This is also consistent with features depicted in some of the schematics described earlier (e.g., Fig. 1b,d,h,k). Fig. 1d, for example, based on steric height (Ridgway and Dunn, 2003), shows east-north-eastward towards the northern tip of New Zealand. This is also consistent with early depictions from Stramma et al. (1995), based on hydrographic measurements. We therefore suggest that the idea of a continuous inertial jet along the Tasman Front (like the Gulf Stream or Kuroshio Extensions) is misleading – and the true pathway is better described as either an eddy train, or a transient current (Fig. 2).

The return flow of the EAC jet, sometimes called the EAC retroflection or the EAC recirculation, was first noted by Hamon (1965), who described the EAC as "U shaped, with a southward current near the continental shelf, and a northward current further offshore". The return flow is a northward flow that appears in mean fields (e.g., Fig. 5; Reid, 1986) and occasionally in synoptic maps (Fig. 3). Consistent with estimates from climatology at 30°S and 32°S (Ridgway and Dunn, 2003; Zilberman et al., 2014), observations from moorings (Mata et al., 2000; Sloyan et al., 2016) at 30°S and 27°S show that the mean meridional flow offshore (from about 200 km from the coast) is northward, accounting for a northward volume transport of 6–16 Sv and a heat transport of 0.24 PW (at 27°S above 2000 m depth). Despite the prominence of the EAC return flow, this important feature of the circulation doesn't always appear in schematics of the circulation of the region (Fig. 1).

One way the EAC differs from other WBCs is the volume transport. The volume transport of the EAC is weaker than other WBCs (e.g., Hogg and Johns, 1995), mainly due to the diversion of some of the Sverdrup transport into the Indonesian Throughflow – as derived from Godfrey's Island Rule (Godfrey, 1989; Godfrey and Dunn, 2010). Various estimates of the transport have been made, typically through geostrophic estimates from hydrographic or XBT surveys (e.g., Nilsson and Cresswell, 1980; Boland and Church, 1981; Ridgway and Godfrey, 1997) and by combining in situ and satellite measurements (e.g., Ridgway et al., 2008, the fields presented in Fig. 6 are an example). Using data from a current meter mooring array, deployed between 1991 and 1993, augmented with hydrographic surveys, Mata et al. (2000) estimated the EAC transport to be approximately 22 Sv, with a standard deviation of 30 Sv. Their array at 30°S at 154.3°E was intended to be upstream of the EAC separation point, however at 30°S they measured significant eddy variability in addition to the boundary current flow. Using a combination of XBT observations and satellite-derived, synthetic temperature and salinity estimates, Ridgway and Godfrey (1994) estimated the EAC transport at 28°S to be 27.4 Sv. Their approach is used to produce the transport estimates presented in Fig. 6. Based on ocean climatology (the CSIRO Atlas of Regional Seas, CARS, Ridgway and Dunn, 2003), Oliver and Holbrook (2014) estimated the EAC transport at 28°S to be 25.8 Sv. More recently, Sloyan et al. (2016) estimate EAC transports from a mooring array near 27°S, where the EAC is now known to be the most coherent (Sloyan et al., 2016). They report that the 18-month period (from April 2012 to August 2013) the mean southward transport above 2000 m was 24.6 ± 6.9 Sv and the net mass transport of -19.25 ± 9.6 Sv (negative indicates a net southward transport). The discrepancy between the southward transport and the net transport is due to northward flow of the EAC recirculation (5.35 Sv) at the eastern end of the mooring array. More recently, Zilberman et al. (2018) combined XBT, Argo, and satellite altimeter data to estimate the EAC transport to be 19.5 ± 2 Sv at around 26°S – noting a typical equatorward return flow of 2.5 ± 0.5 Sv.

Modelling studies show transport estimates similar to observations. For example, in a 14-year regional ocean reanalysis, Schiller et al. (2008) reported that the southward EAC transport at 32°S was 28.7 ± 23.5 Sv. In a 10-year regional modelling study, Kerry et al. (2016;2018) estimated that the southward EAC transport at 30°S was 21.9 ± 31.7 Sv. In a 20-year near-global modelling study, Oke et al. (2013) computed the southward EAC transport off Brisbane to be 21.6 ± 10.6 Sv. In a global ocean model with seasonal surface forcing (and no interannual forcing), Ypma et al. (2016) showed that the mean EAC volume transport at 28°S was 20.4 Sv. Finally, Cetina-Heredia et al. (2015) used a Lagrangian approach to quantify the EAC poleward transport along south-east Australia, and found it to vary from 13.5 ± 7 Sv at 28°S, to 1.04 ± 1 Sv at 39°S. These estimates differ in the period over which they are calculated, and they differ in latitude. Despite this, each estimate is in reasonable agreement with the observational estimates cited above, providing a good indication of the mean EAC volume transport, with observational estimates ranging from 22 to 27.4 Sv, and model-based estimates ranging from 20.4 to 28.7 Sv. Uncertainty in the estimated volume transport tends to grow with latitude moving south, owing to the increased variability in the parts of the western Tasman Sea that are more eddy-rich (south of 27°S).

Sloyan et al. (2016) also estimated the mean southward heat transport above 2000 m to be -1.48 ± 0.44 PW, with a flow-weighted temperature of 15 °C. This highlights the importance of the EAC jet for distributing heat and mass along the coast of south-eastern Australia. Oliver et al. (2017) further demonstrated the importance of the EAC for distributing heat in the ocean, in their report of the so-called "marine heatwave" in the Tasman Sea during Austral summer of 2015/16.

The earliest report of the seasonal cycle of the EAC was from Godfrey et al. (1980). Ridgway and Godfrey (1997) provided a comprehensive analysis of the EAC's seasonal cycle, by showing the seasonal changes in steric height from historical hydrology and XBT data in the EAC region between 25°S and 45°S. They showed that the strongest poleward flow occurs in Austral summer, and that the seasonal amplitude of the EAC volume transport is about 9 Sv, with a minimum in Austral winter. Similarly, Zilberman et al. (2018) used a combination of XBT, Argo, and satellite altimetry data to show that a maximum EAC transport at 26°S of 21.6 ± 1.4 Sv occurs in March, and minimum transport of 18 ± 1.4 Sv in August, in agreement with observations by Wood et al. (2016), who found that only 6% of the variability over the shelf is seasonal. Similarly, Cetina-Heredia et al. (2015) found significant annual variability of the poleward transport between 28 and 39°S, with highest variability evident between 28 and 34°S. The stronger EAC flow in summer is known to be associated with higher Eddy Kinetic Energy (EKE) in the Tasman Sea (Qiu and Chen, 2004) and a poleward shift in the separation latitude (Ypma et al., 2016). Scharffenberg and Stammer (2010) used altimetric Sea Surface Height (SSH) data to investigate the annual cycle in geostrophic velocities and EKE in the global ocean gyres and find a clearer signal in the large-scale circulation rather than in the boundary currents, where the eddy variability dominates. Seasonality of the EAC was also evident in observations of surface velocities from High-Frequency (HF) radar after accounting for the meandering signal associated with eddies (Archer et al., 2017). Over a four year period (2012–2016) the range of the annual cycle of core surface velocity was 0.55 m/s about a mean of -1.35 m/s, between Austral summer and winter at 30–31°S. EKE measured by the HF radar also peaked in summer (dipped in winter), in both magnitude and variance. Throughout the year the EKE/MKE ratio was always below 1, indicating the dominance of the mean flow over eddies at the location of the HF radar, which is centered at 30°S. Archer et al. (2017) also reported that the meandering of the EAC accounted for approximately 50% of the EKE magnitude, but meandering showed no seasonality in variance.

To further investigate the relative magnitude of the mean and transient circulation, we now consider estimates of the EKE/MKE for the EAC region. Sloyan et al. (2016) showed that over the continental slope, the EKE/MKE was less than 1 – but that offshore, the EKE/MKE increased markedly (their Fig. 12). To put these local estimates into

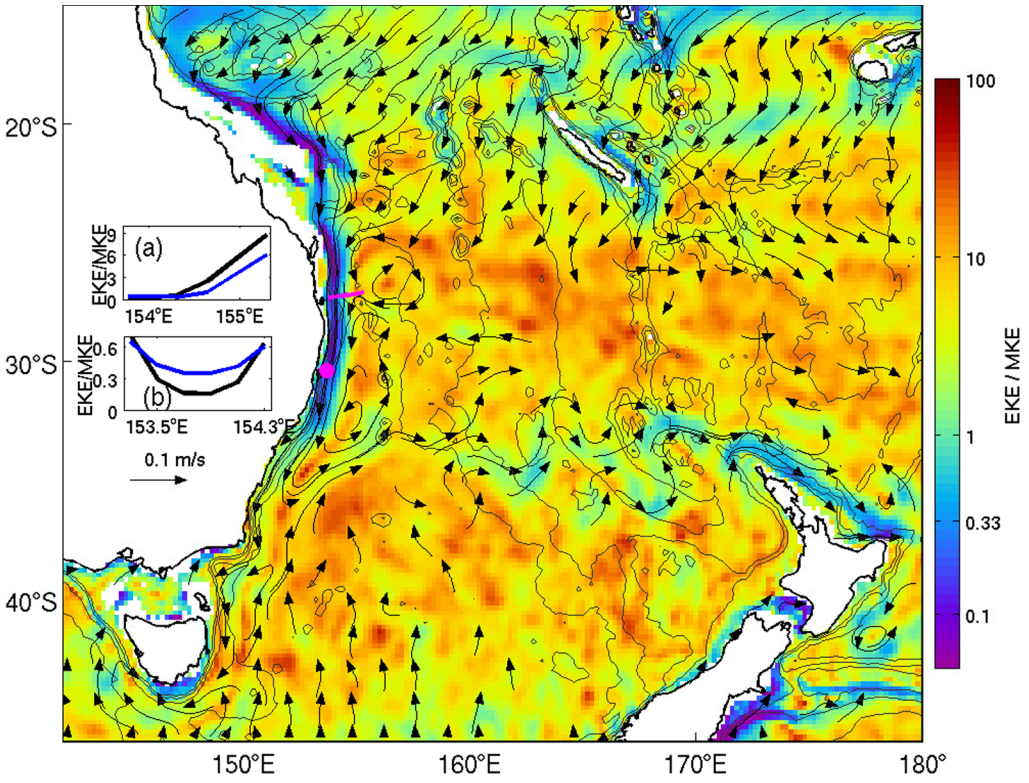

Fig. 8. Ratio of the EKE to MKE (white denotes land or water shallower than 50 m depth) based on altimetry-derived surface geostrophic currents from OceanCurrent analyses (oceancurrent.imos.org.au) for the period 1994–2016. Mean currents from OceanCurrent analyses are shown in vectors, showing only vectors where the speed exceeds 0.1 m/s. The 100, 500, 1000, and 4000 m isobaths are contoured in black. The magenta line denotes the approximate location of the EAC transport array (Sloyan et al., 2016), and the magenta dot shows the approximate location of the Coffs Harbour HF radar footprint (Archer et al., 2017) – both of which calculated EKE/MKE from in situ measurements that are reproduced in the inset panels. Inset (a) compares estimates from Sloyan et al. (2016) (black) and Ocean Current (blue), and inset (b) compares estimates from Archer et al. (2017) (black) and Ocean Current (blue). (For interpretation of the references to colour in this figure legend, the reader is referred to the web version of this article.)

context, we present a map of the time-averaged EKE/MKE[1] for the EAC region, using surface geostrophic velocity estimates from OceanCurrent analysis (oceancurrent.imos.org.au) – based on satellite altimeter observations – in Fig. 8. Included in Fig. 8 are the local estimates by Archer et al. (2017) and Sloyan et al. (2016). The estimates from all data sources considered here are consistent – showing that adjacent to the continental shelf, EKE/MKE is less than 1, but that offshore, EKE/MKE is typically much greater than 1. This means that near the coast, north of about 33°S, the circulation is dominated by the mean flow – that is, the EAC jet dominates. By contrast, offshore, the circulation is dominated by eddies. There is a band of higher EKE/MKE (< 1) across the Tasman Sea between Australia and New Zealand, where the mean current exceeds 0.1 m/s – but this is spatially discontinuous, perhaps suggesting that there is sometimes a zonal flow at different latitudes. This analysis is consistent with the refined picture of the EAC System presented in this review paper – that the EAC is a continuous, meandering stream, flowing adjacent to the continental shelf that "feeds" a field of offshore eddies. Indeed, the EAC stands out among WBCs for its high EKE/MKE ratio (Godfrey et al., 1980). In a recent study, Archer et al. (2018) used high-resolution ocean currents from HF radar data to compare the upstream EAC and Florida Current in the North Atlantic. They found that while the two jets had nearly identical time-mean cross-jet profiles of speed and width, the EAC exhibited significantly higher mesoscale EKE than the Florida Current.

The temperature and salinity of EAC waters also show a seasonal cycle. With sub-tropical origins, the EAC is characterised by warm and salty water (Fig. 9). Throughout the western Tasman Sea, the near-surface waters have a strong seasonal signal, with maximum temperatures ranging from 25 to 28 °C between 25 and 15°S, and ranging from 18 to 23°C between 45 and 35°S. Salinity also changes seasonally between 25 and 15°S, with near-surface waters typically about 0.4 psu fresher in summer owing to increased precipitation. The signature of EAC water in temperature-salinity space is very distinct, with a tight relationship (see the TS diagrams for 145–155°E and 35–25°S in Fig. 9), following a very recognisable "backwards S" shape. Waters below about 26.2 kg/m^3 at mid- and low-latitudes show no seasonal cycle.

The EAC is a baroclinic current that is mostly reported to be surface intensified (e.g., Hamon, 1965; Mata et al., 2006). However, some cross-sections of the EAC have shown a sub-surface velocity maximum at about 100 m depth. This includes observations from a mooring array (Sloyan et al., 2016, Fig. 10d), a ship-board acoustic Doppler current profiler (ADCP, Cresswell et al., 1996, Fig. 10c), from geostrophic current estimates (Huyer et al., 1988; Ridgway and Dunn, 2003), from a diagnostic ocean model (where the model is used to diagnose the three-dimensional velocities from a prescribed field of temperature and salinity – from climatology; Roughan et al. (2003)), and from an idealised modelling study (Gibbs et al., 2000). Observations in Fig. 10 show that the core of the EAC jet often has a maximum at about 100 m depth, with currents that are about 0.2 m/s stronger than they are at the surface. Moreover, Sloyan et al. (2016) reports that during an 18-month deployment there was evidence of a sub-surface maximum 76% of the time (not shown). These results are particularly intriguing, since to date, no physical mechanism to explain the sub-surface maximum has been proposed. However, assuming the thermal wind relationship ($-f\rho_0 \partial v/\partial z = g\partial\rho/\partial x$) approximately holds around the jet (i.e., the flow is approximately geostrophic and hydrostatic), a sub-surface maximum means that $\partial v/\partial z > 0$ above the core of the jet which, by thermal wind, implies that $\partial\rho/\partial x > 0$ (where x and z are the positive to the east and upwards, v is the meridional velocity, f is the Coriolis parameter (negative in the Southern Hemisphere), ρ_0 is the background density, and ρ is density). This indicates that there must be a source of relatively light water near the surface on the shoreward side of the EAC jet. The source of this water is unclear, but we expect it must be either a source of freshwater or surface heating, or a combination of both.

[1] Here, we use the standard Reynolds decomposition: EKE= $(U'^2 + V'^2)/2$ and MKE $=(\overline{U}^2 + \overline{V}^2)/2$, where $U = \overline{U} + U'$ and $V = \overline{V} + V'$ are the zonal and meridional velocities, represented as the sum of the mean, denoted by overbars; and fluctuations, denoted by primes. Using this definition, we implicitly include all variability about the time-mean to represent eddy-variability.

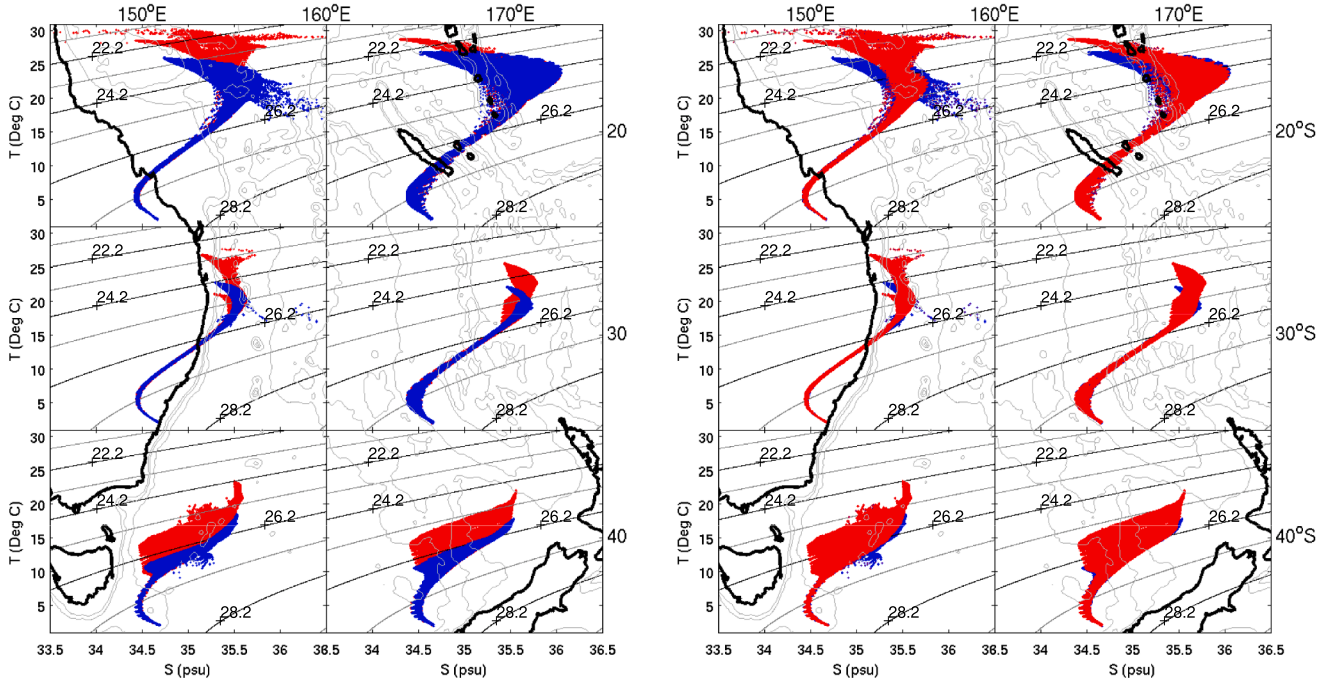

Fig. 9. TS-diagram for 15° × 10° boxes over the Tasman Sea, showing properties from Austral summer (red; using February) and Austral winter (blue; using August), using climatology (Ridgway and Dunn, 2003), with the Australian coastline and topography in the background. The spatial extent of each panel corresponds to the spatial area from which data are used. The data for left and right collection of panels are identical. On the left (right), winter (summer) data are plotted over summer (winter) data to show all the differences clearly. (For interpretation of the references to colour in this figure legend, the reader is referred to the web version of this article.)

3. The EAC separation

The traditional view of the EAC is of a WBC that typically separates from the coast at about 32°S (Godfrey et al., 1980). Interestingly, the first identification of EAC separation was based on the distribution of bottom sediments. Godfrey et al. (1980) noted the absence of fine sediments (indicative of high energy, fast current environments) north of about 32°S. Indications of the EAC separation point from ocean climatology suggest that the EAC typically separates within a range of about 150 km, centred at about 31.5°S (Ridgway and Dunn, 2003). A great number of process studies have been undertaken to understand the dynamics associated with the separation of WBCs from the coast (e.g., Chassignet and Marshall, 2008), however a consensus of the key factors controlling the separation of the EAC from the coast remains somewhat elusive. Unlike other WBCs, the EAC circulation is influenced by the presence of New Zealand. As noted by Warren and Voorhis (1970), the transport from the EAC must somehow "feed" the EAUC – New Zealand's WBC; and the presence of New Zealand also complicates the Sverdrup balance of the South Pacific Ocean.

Adapting the method described by Cetina-Heredia et al. (2014), we objectively identified the separation latitude of the EAC in an eddy resolving ocean model (Masumoto et al., 2004) by first identifying the

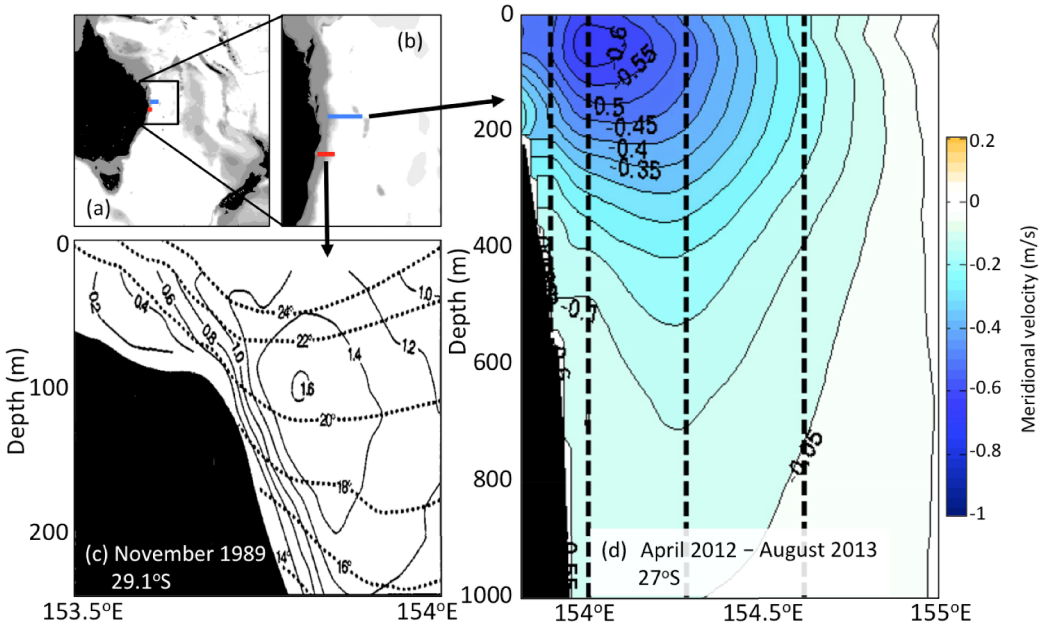

Fig. 10. Sections of meridional velocity from (c) shipboard ADCP data at 29.1°S in November 1989 (adapted from Cresswell et al., 1996), and (d) a time average of moored ADCP data constructed from an 18-month mooring deployment at 27.5°S (adapted from Sloyan et al., 2016, data have been interpolated in space; and dashed vertical lines denote the mooring positions). The approximate section-locations are denoted in panels a and b, where the red line corresponds to panel c, and the blue line to panel d. (For interpretation of the references to colour in this figure legend, the reader is referred to the web version of this article.)

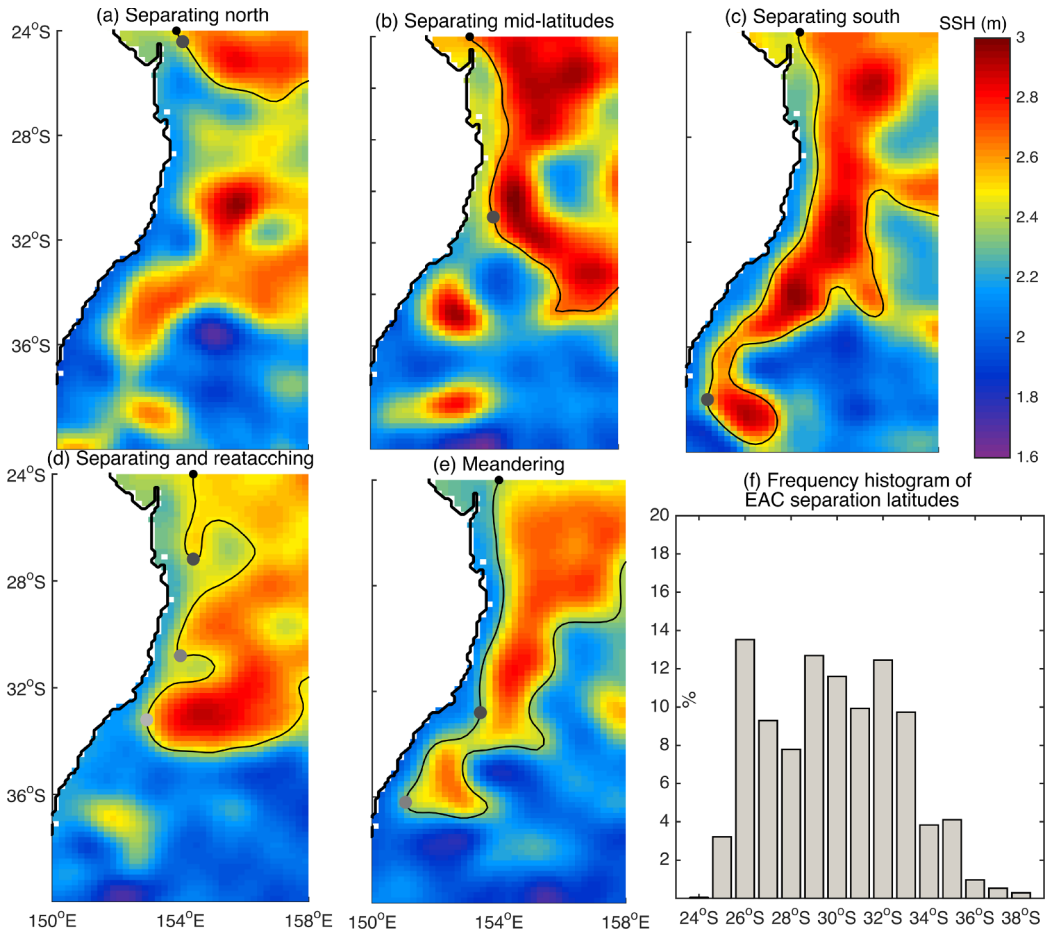

Fig. 11. Examples from AVISO data (Le Traon et al., 2001) showing scenarios when (a–c) the EAC jet separates cleanly from the coast; (d) when the EAC jet separates and then re-attaches; and (e) when the EAC meanders (complicating the estimation of the separation latitude). The bold contour is the line of constant SSH for the value at which the EAC is identified at 24°S. Panel shows a frequency histogram of EAC separation latitudes diagnosed from AVISO data using the method described by Cetina-Heredia et al. (2014).

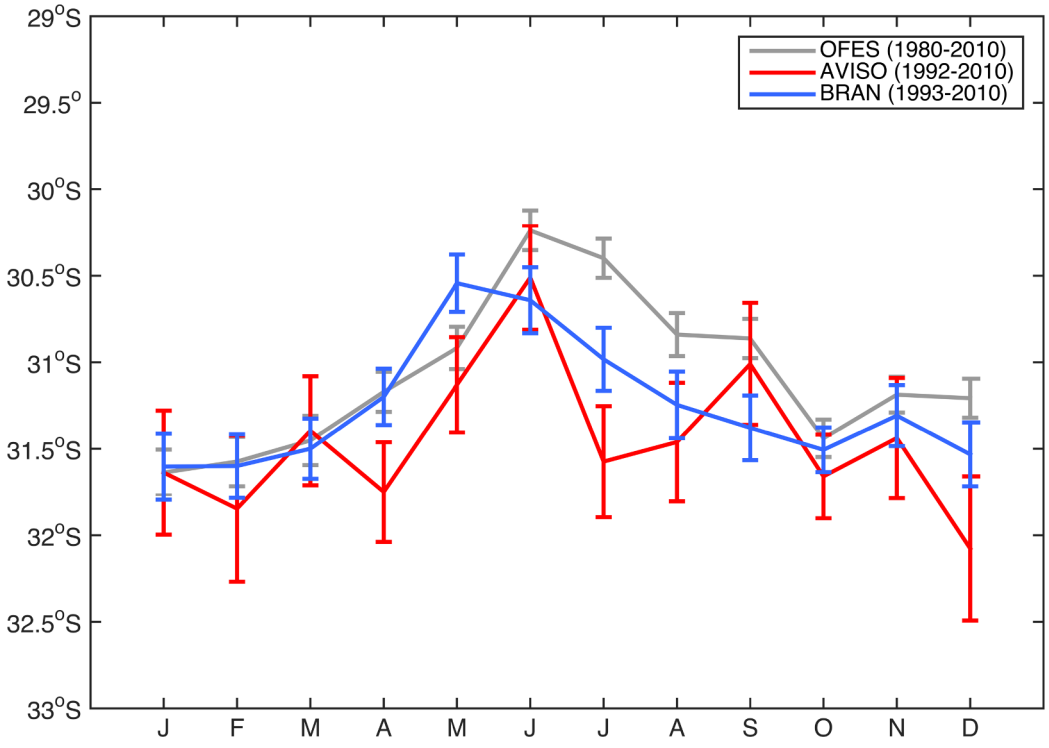

Fig. 12. Seasonal climatology of the EAC separation latitude (mean and standard error) computed from AVISO (Le Traon et al., 2001), OFES (using SSH from a 31-year model run; Masumoto et al., 2004), and BRAN (using SSH from an 18-year ocean reanalysis; Oke et al., 2013) using a method adapted from Cetina-Heredia et al. (2014).

EAC (by the maximum poleward flow) at 28°S and following the corresponding SSH isoline polewards (and equatorwards), along the nominal path of the EAC (see Fig. 11). We recorded the latitude where the EAC deflected from the coast (i.e., when the SSH isoline separated farther than 70 km east of the 150 m isobath), and diagnosed whether it re-attached and separated again at a poleward latitude. Using this

method, we show that the separation latitude of the EAC (Fig. 12) is typically around 31°S, with a seasonal range of about 1.5° of latitude, with the EAC separating from the coast farther to the south in Austral summer. Although the standard error of the estimated means (see the error bars in Fig. 12) for each month is not negligible, the difference between the mean separation latitude in January and June is larger than the standard errors, suggesting that the estimated seasonal cycle is robust (see also, Ypma et al., 2016). Moreover, Cetina-Heredia et al. (2014) explained that the separation of the EAC is strongly linked to the generation and detachment of eddies. This result is consistent with the conclusions of Bowen et al. (2005) and Mata et al. (2006). Analysis of time series of the separation latitude from Archiving Validation and Interpretation of Satellite Oceanographic data (AVISO; Le Traon et al., 2001), for example, shows that over 24 years (1993–2016), the EAC separates from and re-attaches to the coast (e.g., Fig. 11d) at least once along its path no less than 20% of the time (not shown). Furthermore, we find that the EAC can separate as far south as 38°S (e.g., Fig. 11c), and as far north as 24.4°S (e.g., Fig. 11a). The broad latitudinal range over which the EAC separates from the continent reinforces the idea that the EAC is not always a coherent jet but often a meandering poleward stream modulated by eddies.

The temporal and spatial variability of the EAC separation differs from other WBCs (Fig. 4). For example, the Gulf Stream tends to separate consistently at around 35°N, 75°W (Richardson and Knauss, 1971), where the coastline bends eastward. The Agulhas Current generally separates at the southern tip of the Agulhas Bank (37°S, 20.5°E, Harris et al., 1978); and the Kuroshio separates around 35°N, 140°E, also seemingly related to coastline curvature. Nevertheless, the Agulhas separation is also modulated by the formation and detachment of eddies (van Sebille et al., 2009) and the Kuroshio has a well-studied meander that is also related to mesoscale variability (Kawabe, 1995). The Brazil-Malvinas confluence region is also a region of high variability (e.g., Rykova et al., 2017), wth separation positions of the Brazil Current and the Malvinas Current each ranging by about 1000 km (Olson et al., 1988).

A number of factors have been identified as important for influencing the separation of the EAC from the coast. Godfrey et al. (1980) argue that there is likely to be an "inertial overshoot" around 32.5°S causing the southward-flowing EAC to be carried away from the shelf where there is a bend in the coastline to the west. Nilsson and Cresswell (1980) and Godfrey et al. (1980) also suggest that the region of EAC separation may be influenced by Rossby waves propagating westward, across the Pacific Ocean. They suggest that as Rossby waves propagate westward, they are blocked by New Zealand – at about 32°S – and the waves that continue may cause an instability in the EAC when they reach the Australian coastline causing the EAC to separate from the coast. This hypothesis implies that the presence of the New Zealand land mass is an important factor in explaining the latitude of EAC separation. Based on Sverdrup balance, Tilburg et al. (2001) suggested that the largest meridional gradient in the wind stress curl generates an eastward flow at around 34°S that draws the EAC offshore. Moreover, Tilburg et al. (2001) notes that the wind stress curl field over the south Pacific Ocean is unusual, in that it includes a significant decline in the curl but the curl does not drop to zero. Tilburg et al. (2001) suggest that this explains the partial (rather than complete) separation of the EAC jet from the coast. More recently, Bull et al. (2017) and Bull et al. (2018) reported results from a series of numerical experiments with an eddy permitting model that showed that both local wind stress variability, and bathymetry – including the presence of New Zealand – influence mesoscale eddy shedding and consequently the EAC separation. Specifically, they showed that local atmospheric variability increases eddy-shedding rates; and both wind stress variability and absence of New Zealand induce a southward shift of the latitude where the EAC separates. In part, differences in results reported by Bull et al. (2018) and Tilburg et al. (2001) can be explained by differences in the wind products used for each study. Finally, Bowen et al. (2005) and Mata et al. (2006) present evidence supporting the idea that the intrinsic instability of the EAC has been linked to eddy formation that may play a key role in the EAC separation.

There is still no consensus on mechanism, or mechanisms, driving the separation of the EAC jet from the coast. Several studies – both observational (Mata et al., 2000) and modelling (Marchesiello and Middleton, 2000), provided evidence that supports the Rossby wave argument. Other studies have shown the importance of wind forcing and its variability (e.g., Tilburg et al., 2001; Hill et al., 2011; Bull et al., 2017). In fact, Tilburg et al. (2001) disputed the Rossby wave argument, showing that in a linear model forced with monthly climatological winds that either included or excluded New Zealand (with the land masses altered), the EAC still separated from the coast at about the correct location. Nevertheless, using a model that includes non-linear dynamics, Bull et al. (2018) found that in the absence of New Zealand and bathymetric features (>1000 m), the EAC extended farther south before shedding eddies; consequently, its separation latitude had considerably larger variability and its mean was shifted 1° south. In addition, eddies in the EAC separation region are only present when non-linear dynamics are considered. Thus, Bull et al. (2018) argued that the location of the EAC separation was influenced by bottom topography and non-linear effects rather than set solely by the meridional gradients in the wind stress curl. Also, Bostock et al. (2006) presents paleo evidence that suggests that the EAC may have separated between 23 and 26°N during the last glacial maximum, and reports of the continued southward shift of the separation location (e.g., Cai, 2006) seem to discredit the argument for New Zealand's influence on the EAC separation latitude. Bowen et al. (2005) rejected the argument for remote forcing – instead suggesting that local instabilities – perhaps related to intrinsic EAC variability – result in eddy formation that influences EAC separation. The importance of local instabilities is consistent with several other observational and modelling studies (e.g., Mata et al., 2006; Wilkin and Zhang, 2007; Bull et al., 2017). The impact of the coastal alignment – and more generally, the local bathymetry – is supported by several modelling studies (e.g., Oke and Middleton, 2001; Roughan and Middleton, 2002) and by observations (e.g., Schaeffer and Roughan, 2015). Oke and Middleton (2001) and Roughan and Middleton (2002) linked the narrowing of the continental shelf off south-eastern Australia to the alongshore acceleration and separation of the EAC jet. Consistent with this, Cetina-Heredia et al. (2014) showed that the EAC separated most often at latitudes close to narrow points in the continental shelf (either 28.7°S or 30.8°S).

It is likely that all mechanisms referred to above play a role in the EAC separation: Rossby waves, wind stress curl, coastal alignment, bathymetric features, local wind stress variability, and intrinsic instabilities. Perhaps the long-term mean of the EAC separation is constrained by large-scale ocean basin dynamics (i.e., Sverdrup balance and wind stress curl) and features that remained unchanged (e.g., coastal alignment), while variability in shorter time-scales is induced by local dynamics (e.g., local wind stress variability). As in other WBCs (e.g., Schoonover et al., 2017), the explanation for the latitude and variability of the EAC separation seems to be a topic that is still worthy of further investigation.

4. Eddy field

Many studies of the EAC region have analysed statistical properties of the circulation associated with the EAC eddy field. These studies have examined aspects including the rate of eddy shedding (Mata et al., 2006; Bowen et al., 2005; Wilkin and Zhang, 2007); the mechanism of eddy generation (Mata et al., 2006; Ypma et al., 2016); eddy size, intensity, particle-retention, and seasonality (e.g., Qiu and Chen, 2004; Rykova and Oke, 2015; Cetina-Heredia et al. 2019b), eddy path (Pilo et al., 2015b), and other properties (e.g., Everett et al. (2012); Cetina-Heredia et al. (2014); Rykova and Oke (2015); Pilo et al. (2015a); Condie and Condie (2016); Rykova et al. (2017)). Analysis of the

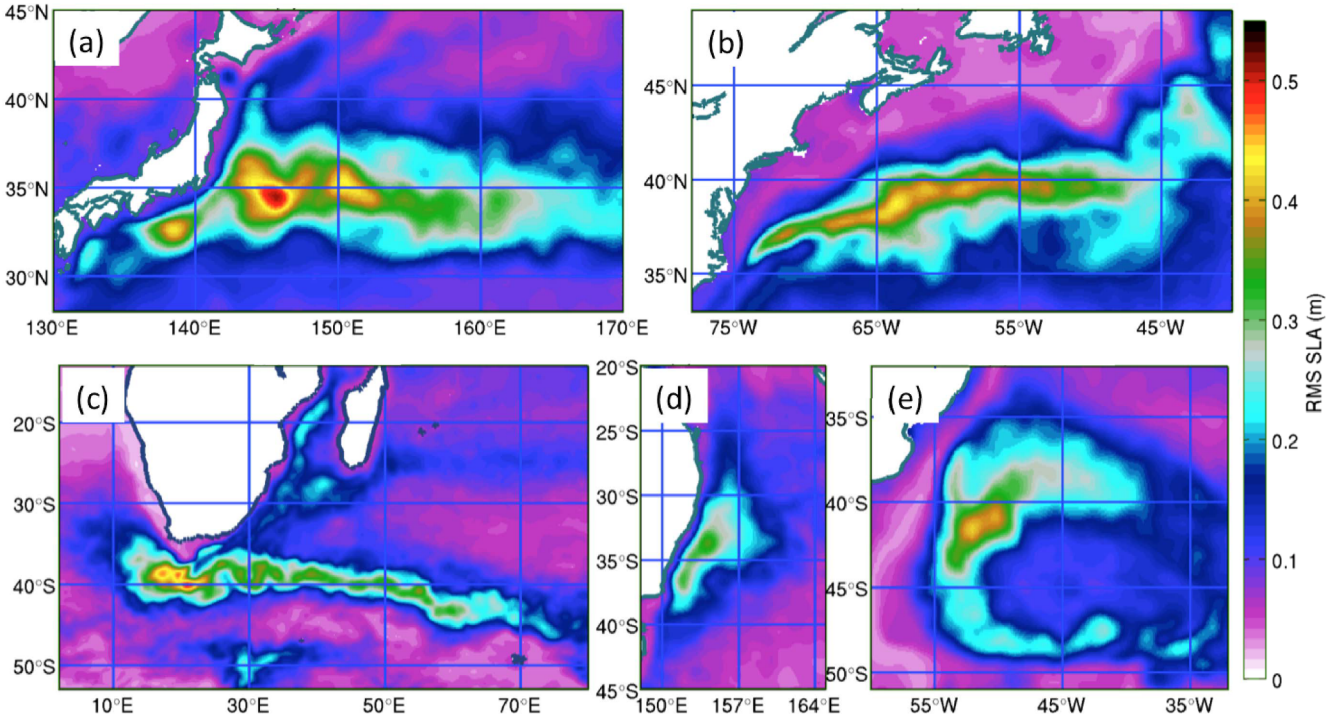

Fig. 13. RMS of the observed SLA for the (a) Kuroshio, (b) Gulf Stream, (c) Agulhas, (d) EAC, and (e) Brazil-Malvinas Confluence region. RMS fields are based on weekly maps of SLA on a 1/3° grid, produced by Archiving, Validation, and Interpretation of Satellite Oceanographic data (AVISO; Ducet et al., 2000). Figure adapted from Oke et al. (2013).

variability in the EAC region – often quantified by the root-mean-square of Sea-Level Anomaly (SLA) or Sea Surface Temperature Anomaly (SSTA), or the EKE shows that the EAC eddy field (Fig. 13d) is energetic throughout the region bounded by the Australian continent to the west and the Lord Howe Rise to the east (e.g., Qiu and Chen, 2004; Mata et al., 2006; Oke et al., 2013; Rykova et al., 2017). This region of high variability extends from about 25°S to 40°S, with a maximum around 33°S. Findings from many of the above-cited studies are outlined below.

The map of the RMS of SLA, described above, is contrasted to other WBC regions in Fig. 13. This comparison shows that the EAC eddy field is energetic in regions where the EAC jet normally flows. In other WBC regions, the regions of relatively large RMS of SLA – denoting the eddy field – are mostly confined to the respective areas after the WBC has "left" the coast. This is true for the Gulf Stream region (Fig. 13b), where high values of the RMS of SLA are mostly along the path of the stream meanders away from the coast and shelf. Similarly, for the Kuroshio (Fig. 13a), the RMS of SLA is high where the Kuroshio meander has separated and after the current separated from the coast (Kawabe, 1995). For the Agulhas Current (Fig. 13c), there is high RMS SLA where the current retroflects, and where it meanders eastwards. The Brazil-Malvinas region shows high RMS SLA only in the vicinity of the confluence (Fig. 13e). As noted, the EAC is quite different to the other WBCs, with high eddy variability along the path of the current while it is still attached to the coast, and also after it separated (Fig. 13d).

Analysis of satellite observations and model results showed that EAC eddies tend to "shed" on time scales of 90–180 days (Bowen et al., 2005; Mata et al., 2006; Wilkin and Zhang, 2007). Similar time scales of variability of the offshore-onshore movement of the EAC jet core were found at 27°S (Sloyan et al., 2016) and 30°S (Archer et al., 2018). Bowen et al. (2005) analysed this apparent timescale using satellite-derived observations south of 27°S and concluded that eddies seemed to originate between 32°S and 35°S. Wilkin and Zhang (2007) used model results to identify two dominant modes of variability in the EAC region – one they attributed to an eddy mode and another to a wave mode. In agreement with Tilburg et al. (2001) and Marchesiello and Middleton (2000), they concluded that the separation of the EAC from the coast was a key to eddy generation in the region. Mata et al. (2006) attributed eddy formation to the coincidence of the "rapid northward migration of the EAC separation point", with a ~100-day period. They clearly demonstrated that the formation of anticyclonic eddies began with a current instability around 25°S. Consistent with all of these studies, analysis of variability in the EAC shows the prevalence of eddies over a broad region (Fig. 13d). EAC eddies spawn regularly, advect with the EAC, merge and coalesce, grow and decay – and often intensify as the EAC jet separates from the coast. Qiu and Chen (2004) clearly showed a distinct seasonality of the EKE associated with the EAC eddy field from satellite observations (their Fig. 5). They showed that eddies originate in all parts of the EAC region, even as far north as 25°S (their Fig. 1) – consistent with logical inferences drawn from Fig. 13d.

The availability of global eddy databases, derived from satellite altimetry (e.g., Chelton et al., 2007; Chelton et al., 2011), has resulted in numerous studies of eddy characteristics. Using one-such database, Everett et al. (2012) identified a region off south-eastern Australia that they call "Eddy Avenue", with particularly biologically productive eddies. Oliver and Holbrook (2014) also demonstrated the prevalence of EAC eddies advecting around southern Tasmania, and van Sebille et al. (2012) showed that eddy-propagation explained up to 46% (17% in cyclonic eddies and 29% in anticyclonic eddies) of the volume transport of the EAC "leakage". Furthermore, Pilo et al. (2015b) showed that up to 30% of large anticyclonic eddies generated in the EAC region follow this path, with some eddies lasting for 5 years and travelling distances of thousands of kilometres. As EAC eddies propagate southwards, they contribute to the poleward transport of EAC waters. Cetina-Heredia et al. (2014) showed that transport within eddies can explain up to 60% of the net southward transport – which has increased between 1980 and 2010, particularly from 2005 onwards. Other properties of EAC eddies are also changing. For example, Rykova and Oke (2015) combined satellite observations with Argo profiles to better understand the structure and variability of EAC eddies. They showed that between 2005 and 2012, EAC eddies have freshened by 0.17–0.25 psu/decade –

a finding that they attribute to increased precipitation in the western, subtropical South Pacific – although the short duration of their time series doesn't rule out some sort of decadal variability (rather than a freshening trend).

Some recent studies have analysed results from large-scale eddy-resolving models to better understand eddy variability in the EAC region. For example, Rykova et al. (2017) contrasted eddy structure in the EAC region to other WBC regions. They showed that although EAC eddies tend to be weakest in terms of associated velocities and vertical heave of isopycnals (compared to eddies in the Kuroshio, Gulf Stream, Agulhas, and Brazil-Malvinas regions), they are also the least variable and the most baroclinic.

Although out of scope for this paper, we note that the impact of eddies on the coastal ocean and cross-shelf transport has been widely examined (e.g., Suthers et al., 2011; Schaeffer and Roughan, 2015; Wood et al., 2016; Schaeffer et al., 2017, and references therein). In addition, progress has been made on quantifying how eddies contribute to the productivity of the region through their ability to entrain, retain and sustain larval fish (e.g., Mullaney et al., 2011; Everett et al., 2015; Macdonald et al., 2016; Roughan et al., 2017).

5. Structure of EAC eddies

As noted in Section 1, there has been a recent resurgence in the study of individual eddies in the EAC region (e.g., Oke and Griffin, 2011; Pilo et al., 2015a,b, 2018; Roughan et al., 2017). Findings from these studies have led to recognition of the importance and complexity of the vertical structure of eddies, the circulation within eddies, the vertical tilt of eddies, the path and longevity of eddies, and the prevalence of different types of eddies. Some key findings from these studies, along with a reminder of the early learnings of such studies, are described below.

The pioneering studies of EAC eddies delivered understanding of how eddies form (e.g., Nilsson and Cresswell, 1980; Rochford, 1983) and stack during merging events (e.g., Nilsson and Cresswell, 1980), about seasonal surface flooding (e.g., Cresswell, 1983; Tranter et al., 1982), velocities (and level of no-motion) within eddies (Hamon, 1965; Boland and Hamon, 1970), and eddy propagation (e.g., Hamon, 1965). All of these early studies were based on analysis of limited in situ measurements, reporting details of individual eddies. Findings from each study were described without too much generality – but often with very insightful inference. Many of the insights described by the above-mentioned pioneering scientists, have since proven to be very accurate.

Velocities in eddies are strong, with reported values of up to 2 m/s (Nilsson and Cresswell, 1980). Analyses of model results and altimetry-derived fields indicate that velocities associated with EAC eddies are typically about 0.5–0.6 m/s, surface intensified, with coherent currents (weaker at depth) over the full water column (Everett et al., 2012; Rykova et al., 2017, Figure 14). Consistent with this, Mulhearn et al. (1988) reported measurements of abyssal velocities with fluctuations that were consistent with the passage of eddies. Typical anticyclonic EAC eddies have a sub-surface maximum in salinity – with values exceeding 35.6 psu – at around 150–200 m depth; and vertically displaced isopycnals of about 250 m (Rykova et al., 2017). Cyclonic EAC eddies tend to be weaker than anticyclonic eddies, and often much smaller (Everett et al., 2012; Rykova et al., 2017), with currents of about 0.45–0.5 m/s and vertically displaced isopycnals of about 190 m (Rykova et al., 2017). EAC eddies always have a clear signature in SLA – with anticyclonic eddies characterised by positive SLA of around 0.25 m (Everett et al., 2012), but sometimes as large as 0.8 m (Rykova et al., 2017); and cyclonic eddies characterised by SLA of around −0.25 m, and sometimes as large as −0.6 m. By contrast, EAC eddies do not always have a clear signature in satellite SST (e.g., Bowen et al., 2005; Rykova et al., 2017). Anticyclonic eddies in the EAC region usually show a positive SST anomaly (Everett et al., 2012; Rykova et al., 2017), but cyclonic eddies sometimes have no surface signature in SST (Fig. 14, Rykova et al., 2017). The main reason for this seems to be due to surface flooding (e.g., Baird and Ridgway, 2012).

Surface flooding of eddies occurs when the warm, light waters of the EAC jet partially flow over the top of (over-wash) an eddy (Tranter et al., 1982; Baird and Ridgway, 2012; Macdonald et al., 2013). As a result, the cyclonic eddies are sometimes undetectable in satellite SST. Despite this lack of a surface signature, the underlying flooded eddy has properties of surface-intensified eddies. Similar to surface flooding, anticyclonic eddies can also "sink" under other anticyclonic eddies after cooling (Tranter et al., 1982; Nof and Dewar, 1994; Baird and Ridgway, 2012). Using observations from a number of different platforms, Baird et al. (2011) described the dynamics of such an event, in which a shallow layer (~60 m) of warm, fresh EAC waters encircled an anticyclonic eddy resulting in a deep isothermal layer. Their results were reminiscent of the stacking of eddies in the EAC region reported by Cresswell (1983) and Cresswell and Legeckis (1986).

An example of recent observations showing evidence of stacked EAC eddies is presented in Fig. 15a. In this example, temperature and salinity profiles from a single Argo float show evidence of the two mesoscale eddies merging (Fig. 15a) – with water from one eddy moving over the top of another. In September 2009, an Argo float sampled a strong anticyclonic eddy with a deep surface mixed layer. The Argo float moved out of the eddy for a few weeks in November 2009 – apparently during an eddy-merging event – before moving back into the resultant stacked eddy with two distinct mixed layers. The surface mixed layer spans the top 400 m of the water column with characteristics that match the original eddy; and the second mixed layer spans depths of 500–900 m. The Argo float remains in the double-core eddy for several months until April 2010 – returning fascinating data of the eddy evolution. The double-core eddy has large temperature and salinity anomalies between the surface and almost 1200 m depth (Fig. 15a). Glider observations in the same region for a different period also show evidence of a double-core eddy. This is not the first time that evidence of stacked EAC eddies has been described. Cresswell (1982) presented a similar case study from observations collected in 1981 (Fig. 15b). The prevalence of such events in the EAC remains unclear.

In a modelling study with data assimilation Oke and Griffin (2011) analysed the development and evolution of a large-amplitude cyclonic EAC eddy. They noted that the cyclonic eddy had a significant tilt, where the property anomalies and circulation of the eddy (e.g., the eddy centre, identified as the local minimum in the horizontal current speed) were not aligned vertically, with mis-alignment of up to 60 km at 1000 m depth. Eddy tilting has been previously seen in other regions (e.g., Roemmich and Gilson, 2001) – but the study by Oke and Griffin (2011) was the first acknowledgement of this characteristic in the EAC region. Subsequently, Roughan et al. (2017) intensively observed (sampled at high spatial resolution) two contrasting cyclonic eddies and also noted a significant tilt. This titling is thought to influence the biological productivity around an eddy – with potentially nutrient-rich water not only transported horizontally around the eddy, but also vertically – perhaps in and out of the surface mixed-layer and euphotic zone (see Oke and Griffin (2011)). Additionally, we expect that the tilting of eddies is likely to influence the water mass exchange within the eddy and its energetics. These recent findings lead us to speculate that many (perhaps most) EAC eddies have a tilt – but also note that the mechanisms resulting to tilting are not well understood.

The widely-accepted conceptual model of vertical velocity within eddies is of an upward (downward) flow at the centre of cyclonic (anticyclonic) eddies, as depicted schematically by McGillicuddy et al. (1998). While this picture must be true when an eddy first forms, or as they rapidly intensify – as noted by Flierl and McGillicuddy (2002) – it is unclear whether this occurs in "mature eddies". Vertical velocity cannot be reliably measured from observations, so studies of the vertical velocities associated with eddies have almost exclusively been based on model results. Several studies of individual eddies have reported the vertical velocities of EAC eddies (e.g., Oke and Griffin, 2011)

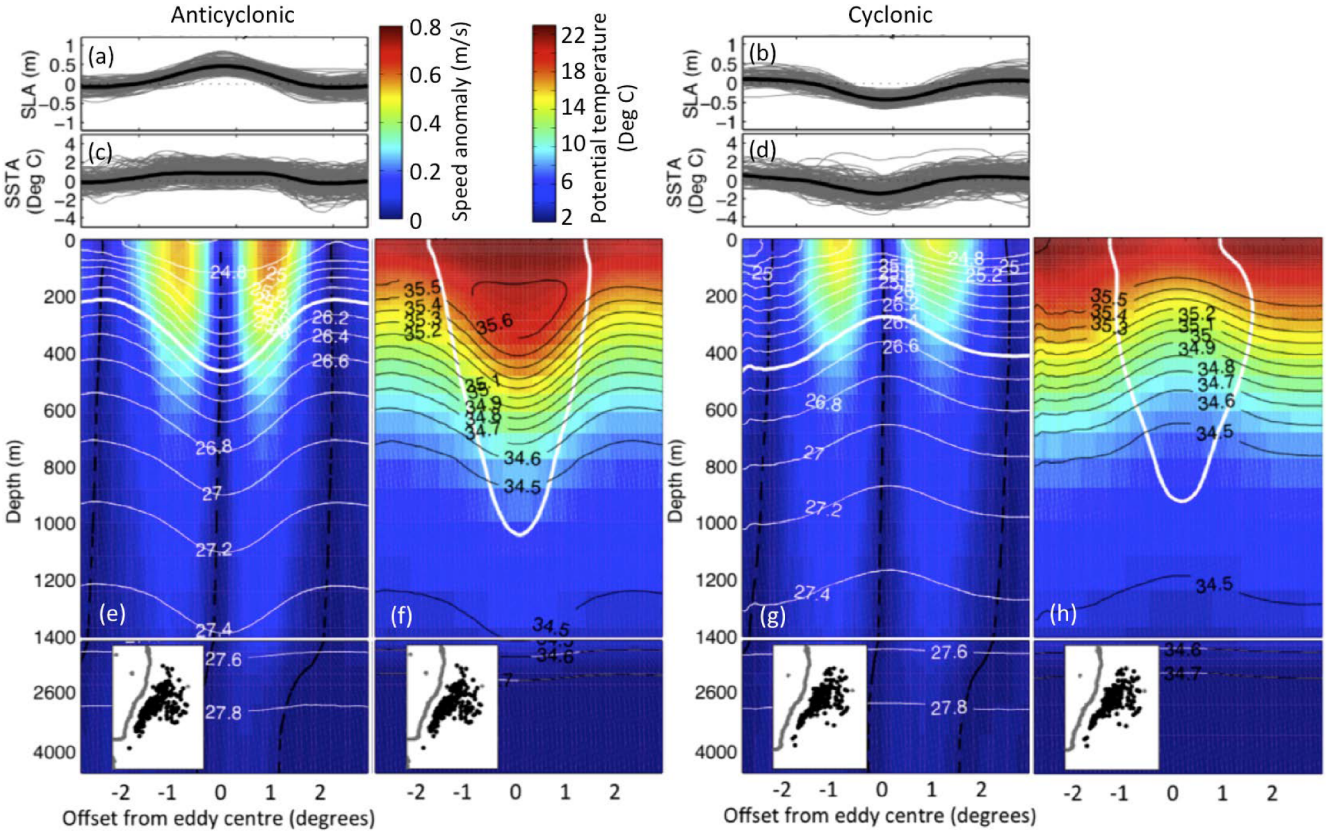

Fig. 14. Mean (black) and individual (gray) cross-sections of SLA (a,b), SSTA (c,d), speed anomaly (e, g; colour), potential density (f, h; white contours), the zero velocity contour (e, g; bold black contour), mean potential temperature (f, h; colour) and salinity (f, h; black contours), and the 0.1 kg/m^3 potential density anomaly contour (f, h; white contour) from 216 anticyclonic (left; a, c, e, f) and cyclonic (right; b, d, g, h) eddies from an eddy-resolving ocean model (Oke et al., 2013) in the EAC region. The inserts in panels e-h show the locations of the 216 manually-identified eddy centres. Adapted from Rykova et al. (2017). (For interpretation of the references to colour in this figure legend, the reader is referred to the web version of this article.)

– but none have reported results consistent with McGillicuddy's conceptual model. Rather, Oke and Griffin (2011) described an example with large vertical velocities around the perimeter of a cyclonic eddy that they assumed to be related to eddy tilt. Pilo et al. (2018) investigated the vertical velocities of EAC eddies in more detail, showing that many long-lived (up to 5-years), large-amplitude, anticyclonic eddies have four local extrema around each eddy – with a quad-polar pattern (e.g., Fig. 16). Pilo et al. (2018) showed that this feature of eddies was caused by "eddy distortion", where an eddy changes shape (becoming more or less isotropic). Schaeffer et al. (2017) reported observations of frontal eddies from high-resolution HF radar data off Coffs Harbour, noting evidence of enhanced nutrient enrichment in the vicinity of these small (sometimes just 10 km radius), but energetic eddies. This fascinating picture of the vertical circulation associated with eddies is evident in fields of data-derived vertical velocity (Nardelli, Oct 2013) and in idealised modelling studies in other regions (Martin and Richards, 2001); but the prevalence of these patterns in EAC eddies is unclear.

Lens-type eddies in the EAC region were first observed in the 1980s (e.g., Cresswell (1983) and Cresswell and Legeckis (1986)), and have again been the focus of a number of studies of individual eddies in recent years. Using glider data, Baird and Ridgway (2012) showed three lens-type anticyclonic eddies off eastern Australia (Fig. 17). These eddies have a subsurface core, between 400 and 600 m depth, and carry a patch of Bass Strait Water in their interior. Using results from an eddy-resolving ocean model, Pilo et al. (2015b) showed that sometimes surface-intensified eddies, formed near the EAC separation point, subduct as they propagate southwards. Pilo et al. (2015b) presented examples where such eddies propagate around Tasmania and towards the Indian Ocean – retaining lens-type properties for several years. We note that details of the subduction process in EAC eddies remains poorly understood.

Few studies of individual EAC eddies have focused on eddy particle retention. Using data from two drifting buoys trapped in an EAC anticyclonic eddy for 60 days, Brassington (2010) described the time evolution of eddy surface divergence. The buoys converged on four separate occasions during the time period, before being finally ejected after an eddy merging event (Brassington et al., 2011). Condie and Condie (2016) estimate eddy retention time scales across a range of oceanic environments including two cyclonic eddies and one anticyclonic eddy within the EAC System. They found retention times of modelled plankton within these eddies ranged from 13 to 40 days. Although some effort has been made quantifying retention by individual eddies, a systematic approach to understand retention by eddies in this region is lacking.

6. Interannual and decadal variability

Consistent with reports of warming in WBCs around the world (Wu et al., 2012), a 60-year time series of temperature off eastern Tasmania shows variability with a quasi-decadal period and a positive long-term trend (Fig. 18). This supports the assertion in several studies that the South Pacific sub-tropical gyre has spun up since the 1990s (Roemmich et al., 2007, who analysed 1993-2004), resulting in an increase in the volume transport of the EAC jet (Ridgway et al., 2008, considering 1995–2001) that appears related to changes in the basin-wide wind stress field (Oke and England, 2004; Cai, 2006; Roemmich et al., 2007; Hill et al., 2008; Oliver and Holbrook, 2014). Some studies have

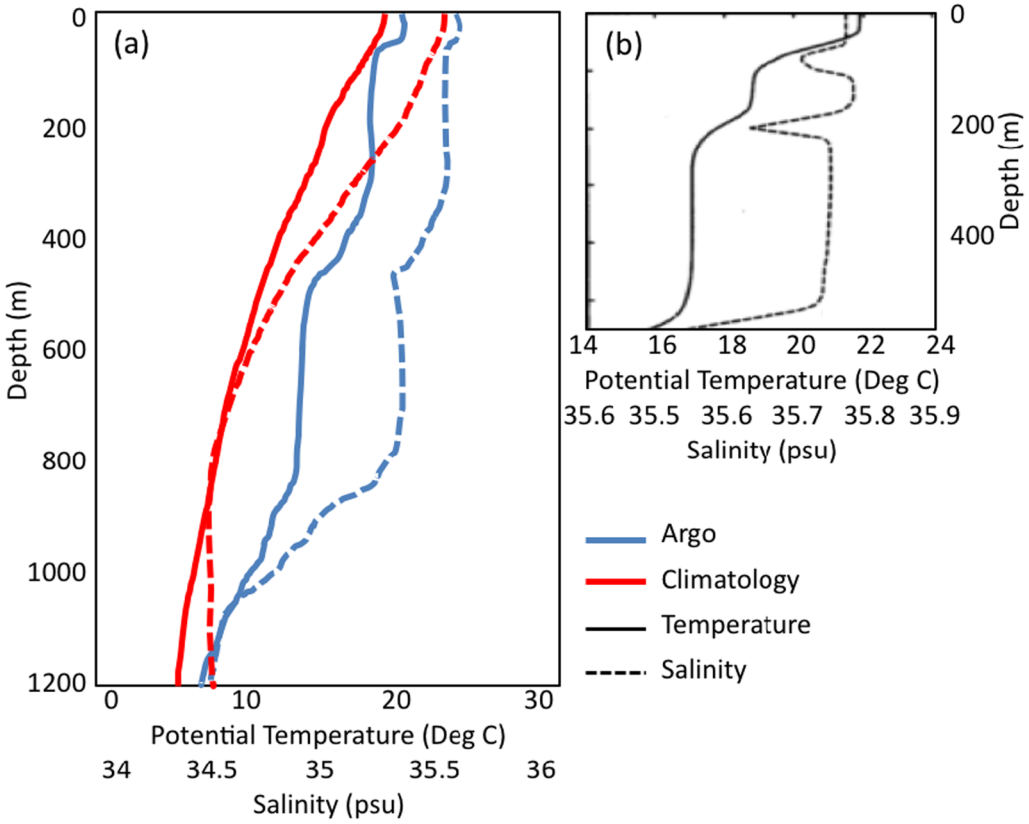

Fig. 15. Examples of profiles of potential temperature (solid) and salinity (dashed) from Argo (blue, panel a), climatology (red, panel a), and CTD (panel b) showing stacked eddies after the merging of two anticyclonic EAC eddies in (a) April 2009 and (b) April 1981 (panel b adapted from Cresswell, 1982). (For interpretation of the references to colour in this figure legend, the reader is referred to the web version of this article.)

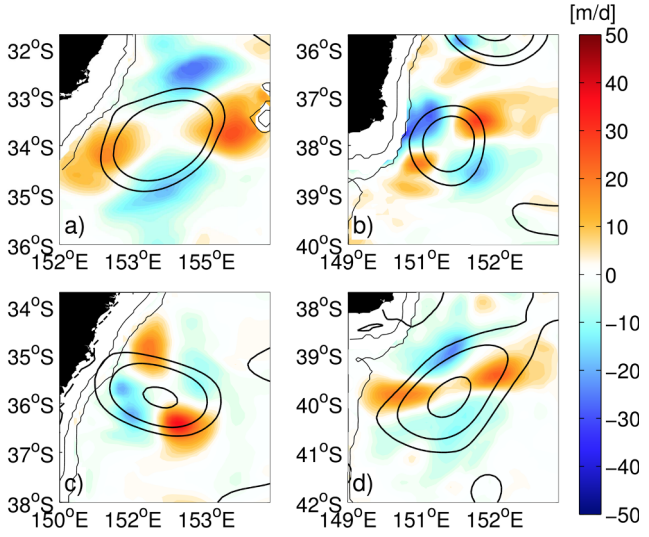

Fig. 16. Daily mean fields of depth-averaged (0–2000 m) vertical velocity in an anticyclonic eddy in the EAC region from a near-global, eddy-resolving ocean model (Oke et al., 2013); adapted from Pilo et al. (2018). The bold black lines are the 0.1, 0.25 and 0.5 m SLA contours, and the thin black lines are the 1000 and 3000 m isobaths.

attributed the changes in the gyre strength and location (noting a poleward shift) to changes in the wind stress curl (e.g., Oke and England, 2004; Cai, 2006; Roemmich et al., 2007), and some have linked changes in frequency and intensity of Rossby waves to the EAC transport and separation (Hill et al., 2008; Holbrook et al., 2011). Some studies suggested that the "gating" between flow along the "Tasman Front" and the "EAC Extension", as described in Section 2, varies on decadal and longer time-scales (Hill et al., 2011; Oliver and Holbrook, 2014; Sloyan and O'Kane, 2015). Cetina-Heredia et al. (2014) found that the mean latitude of the EAC separation has shifted poleward by about 70 km since the 1980s, but that the range of latitudes where the EAC separates (which extends over about 1000 km) has not changed.

Ridgway (2007) concluded that the interannual variability of the EAC System is unrelated to ENSO, but others have suggested that there is a weak but significant correlation between the EAC transport and separation latitude and variability in the tropical Pacific (e.g., Cetina-Heredia et al., 2014). This discrepancy warrants further investigation.

Consistent with the reports of the strengthening of the EAC jet, reported above, there is evidence that EAC eddies are transporting more water poleward (Cetina-Heredia et al., 2014). Specifically, (Cetina-Heredia et al., 2014, their Figure 9c) show that eddies (both cyclonic and anticyclonic) account for 5–19% of the southward transport of the EAC – with an abrupt increase between 2005 and 2010 (their study spanned 1980–2010). There is also evidence that the properties of EAC eddies are changing, with Argo observations showing that between 2005 and 2012 eddies have freshened at a rate of about 0.02 psu/year and have no significant temperature change (Rykova and Oke, 2015).

The EAC System clearly varies on interannual and decadal time scales, but how it will change in the future is unclear. Climate projections, using coarse-resolution models suggest that the EAC jet will strengthen, resulting in warming in the south Tasman Sea (Cai et al., 2005). Some eddy-resolving climate downscaling studies have also been undertaken (Chamberlain et al., 2012; Sun et al., 2012), suggesting that we might expect stronger transports along the path of the EAC Extension, and a more energetic eddy field (Matear et al., 2013; Oliver and Holbrook, 2014). It's likely that downscaling will continue to be important, since the coarse models used for climate projections don't resolve the key elements of the EAC System, namely the EAC separation, path, and its eddies. Analysis of ocean observations, like that of Rykova and Oke (2015), for contemporary periods will also play a role in the early detection of changes to the EAC System.

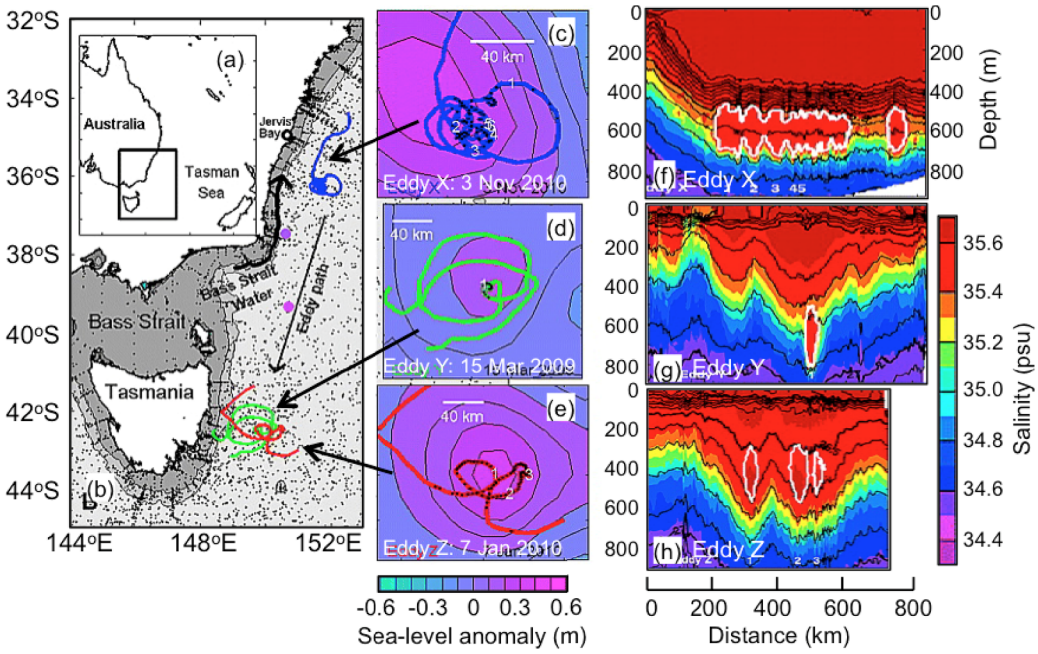

Fig. 17. Observations from gliders showing properties of lens-type EAC eddies. (a) Regional map; (b) schematic, including glider tracks (colours) for three deployments, spanning 3–6 months during 2009–2010; (c–e) maps of SLA, with glider tracks overlaid; (f–h) cross-sections of salinity along each glider path. Adapted from Baird and Ridgway (2012). (For interpretation of the references to colour in this figure legend, the reader is referred to the web version of this article.)

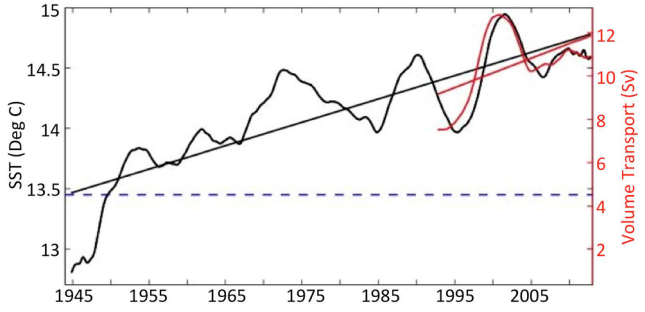

Fig. 18. Time-series of low-passed filtered SST from the Maria Island station (left axis, black line); and southward volume transport off eastern Tasmania, estimated from satellite altimetry (right axis, red line). The Maria Island SST and EAC transport trends in black and red curves respectively. The blue dashed line indicates the observed trend SST and the inferred EAC transport in 1944. (For interpretation of the references to colour in this figure legend, the reader is referred to the web version of this article.)

7. Conclusion

Despite decades of research, there is still wide-spread misunderstanding about the typical ocean circulation in the EAC region (Fig. 1). This is reminiscent of the early pontification of Hamon (1980), who authored an article entitled, "The East Australian Current – continuous, or a series of eddies?" In this review paper, we present a refined picture of the EAC System that reflects new and old understanding of the region. Consistent with the early speculation and inference of Hamon (1980) and Godfrey et al. (1980), and the evidence from more recent observations and models, we suggest that the EAC System consists of the EAC jet and a field of eddies, extending southwards and around Tasmania, and across the Tasman Sea towards New Zealand – feeding the East Auckland Current. The EAC is a meandering, poleward flow that becomes a complex field of eddies that decay, merge, and advect (Fig. 2). We show that this contrasts with other WBCs (e.g., Fig. 4), where a long, continuous, offshore stream is often present (e.g., Gulf Stream Extension). For the EAC, we observe that at no point in time is there evidence of a continuous, coherent flow along either the Tasman Front (Andrews et al., 1980) – towards New Zealand – or the EAC Extension – around Tasmania (Ridgway and Dunn, 2003). Rather, we show that these features only appear in time-averages of the circulation, or as a train of eddies. This picture of the EAC refines the many different views of the EAC, as represented in many published schematics (Fig. 1), where it is implied that the Tasman Front and the EAC Extension are features of the EAC System that are present as continuous, semi-permanent streams. We present evidence to support this view from both observations and models.

Another aspect of the EAC System that differs from other WBCs is the co-location of eddies to the EAC jet. We show that eddies are typically present along the entire path of the EAC jet (e.g., Fig. 13) – not just after the EAC jet separates from the coast. By contrast, for other WBCs, an energetic eddy field (evident in high EKE or high sea-level variance) is restricted to the regions where the WBC flows offshore (e.g., Gulf Stream or Kuroshio Extensions). Unlike other WBCs, the EAC System is also strongly influenced by role of the ITF, the presence of New Zealand, and unique aspects of the wind stress curl over the South Pacific Ocean. These elements rendering the EAC as the weakest of all WBCs.

For the first time, we now have some observations of the full depth of the EAC (Sloyan et al., 2016), however there is still work to be done in characterising the variability of the EAC and understanding of the dynamics of the EAC jet itself. For example, observations show that the EAC jet sometimes has a sub-surface velocity maximum. But a dynamical explanation for this feature has not been proposed and reproduction of the sub-surface maximum in models is uncommon (with few exceptions: Gibbs et al., 2000; Roughan et al., 2003). By contrast, we note that most modelling studies show a surface-intensified flow associated with the EAC jet. We also do not know the prevalence and spatial extent of the sub-surface core. This warrants further investigation.

Despite the progress that we have made in our understanding of the EAC System, we still do not fully understand the mechanisms driving the separation of the EAC jet from the coast. In this review, we refer to many studies that propose different mechanisms that influence separation. For each mechanism, there is convincing evidence in the published literature that supports each argument. We therefore suggest that most – perhaps all – of the cited mechanisms play a role at different times. This aspect of the EAC System needs more investigation.

We also describe and provide comments on recent work on the EAC region, with reference to early studies of the EAC and its eddies. Arguably, the most progress over the past decade has been made in our

understanding of EAC eddies themselves. We now have significant insight into their shedding frequency, lifespan, water-mass characteristics, mean paths, and their three-dimensional structure. While recent modelling (Oke and Griffin, 2011) and observational (Roughan et al., 2017) studies have shown that eddies tilt within the EAC System, and we speculate that many (perhaps most) EAC eddies tilt, the dynamics that drive eddy-tilting and the asymmetric three-dimensional structure (and depth extent) are not well understood. Similarly, a complete picture of what factors influence the instabilities responsible for eddy generation is unavailable – though we note that Bowen et al. (2005) and Mata et al. (2006) provide strong evidence for EAC instabilities originating upstream of the EAC, rather than propagating westward from offshore. This means that prediction of the EAC eddy field remains a challenge. Coincidentally, the region of highest eddy variability lies adjacent to Australia's most populated coastline, where societal impacts are the greatest. This should motivate continued research on these important aspects of the regional ocean circulation.

Acknowledgements

We sincerely acknowledge and thank the role of the Anonymous Reviewers of this manuscript. The reviews we received were challenging, constructive, extensive, and insightful. In addressing the Reviewers' comments, we believe this manuscript has improved significantly. Data was sourced from the Integrated Marine Observing System (IMOS, www.aodn.org.au). IMOS is a national collaborative research infrastructure, supported by the Australian Government. Argo data were collected and made freely available by the International Argo Program and the national programs that contribute to it (www.argo.ucsd.edu, argo.jcommops.org). The Argo Program is part of the Global Ocean Observing System. Satellite altimeter data is provided by NASA, NOAA, and CNES. SST observations are provided by NOAA (www.nodc.noaa.gov) and Remote Sensing Systems (www.remss.com). Model data used in this study are from the Bluelink suite of global models, and from OFES. The authors gratefully acknowledge M. Felsing and MetOcean Solutions, New Zealand, for hosting the 2017 EAC writing workshop – where this review paper was conceived and first drafted. We also wholeheartedly thank our colleagues and peers who have worked tirelessly to advance our understanding of the EAC System.

Appendix A. Supplementary material

Supplementary data associated with this article can be found, in the online version, at https://doi.org/10.1016/j.pocean.2019.102139.

References

Andrews, J.C., Lawrence, M.W., Nilsson, C.S., 1980. Observations of the Tasman front. J. Phys. Oceanogr. 10 (11), 1854–1869.
Andrews, J.C., Scully-Power, P., 1976. The structure of an East Australian Current Anticyclonic Eddy. J. Phys. Oceanogr. 6 (5), 756–765.
Archer, M.R., Keating, S.R., Roughan, M., Johns, W.E., Lumpkin, R., Beron-Vera, F., Shay, L.K., 2018. The kinematic similarity of two western boundary currents revealed by sustained high-resolution observations. Geophys. Res. Lett. 45. https://doi.org/10.1029/2018GL078429.
Archer, M.R., Roughan, M., Keating, S.R., Schaeffer, A., 2017. On the variability of the East Australian Current: jet structure, meandering, and influence on shelf circulation. J. Geophys. Res.: Oceans 122 (11), 8464–8481.
Baird, M.E., Ridgway, K.R., 2012. The southward transport of sub-mesoscale lenses of Bass Strait Water in the centre of anti-cyclonic mesoscale eddies. Geophys. Res. Lett. 39 (2).
Baird, M.E., Suthers, I., Griffin, D.A., Hollings, B., Pattiaratchi, C.B., Everett, J.D., Roughan, M., Oubelkheir, K., Doblin, M.A., 2011. The effect of surface flooding on the physical-biogeochemical dynamics of a warm-core eddy off southeast Australia. Deep Sea Res. 58 (5), 592–605.
Black, A., 1853. Black's General Atlas of the World. Adam and Chales Black, Edinburgh.
Boland, F., Church, J., 1981. The East Australian Current 1978. Deep Sea Res. Part A Oceanogr. Res. Papers 28 (9), 937–957.
Boland, F., Hamon, B., 1970. The East Australian Current, 1965–1968. Deep Sea Res. Oceanogr. Abstr. 17 (4), 777–794.
Bostock, H.C., Opdyke, B.N., Gagan, M.K., Kiss, A.E., Fifield, L.K., 2006. Glacial/interglacial changes in the East Australian Current. Clim. Dyn. 26 (6), 645–659.
Bowen, M.M., Wilkin, J.L., Emery, B., 2005. Variability and forcing of the East Australian Current. J. Geophys. Res. 110 (C3), C03019.
Brassington, G.B., 2010. Estimating surface divergence of ocean eddies using observed trajectories from a surface drifting buoy. J. Atmosph. Oceanic Technol. 27 (4), 705–720.
Brassington, G.B., Summons, N., Lumpkin, R., 2011. Observed and simulated Lagrangian and eddy characteristics of the East Australian Current and the Tasman Sea. Deep Sea Res. 58, 559–573.
Bull, C., Kiss, A.E., Jourdain, N.C., England, M.H., van Sebille, E., 2017. Wind forced variability in eddy formation, eddy shedding, and the separation of the East Australian Current. J. Geophys. Res.: Oceans 122, 9980–9998.
Bull, C.Y., Kiss, A.E., van Sebille, E., Jourdain, N.C., England, M.H., 2018. The role of the New Zealand plateau in the Tasman Sea circulation and separation of the East Australian Current. J. Geophys. Res.: Oceans 123 (2), 1457–1470.
Cai, W., 2006. Antarctic ozone depletion causes an intensification of the Southern Ocean supergyre circulation. Geophys. Res. Lett. 33 (3).
Cai, W., Shi, G., Cowan, T., Bi, D., Ribbe, J., 2005. The response of the Southern Annular Mode, the East Australian Current, and the southern mid-latitude ocean circulation to global warming. Geophys. Res. Lett. 32 (23).
Carton, J.A., Giese, B.S., 2008. A reanalysis of ocean climate using Simple Ocean Data Assimilation (SODA). Monthly Weather Rev. 136, 2999–3017.
Cetina-Heredia, P., Roughan, M., Sebille, E., Feng, M., Coleman, M.A., 2015. Strengthened currents override the effect of warming on lobster larval dispersal and survival. Global Change Biol. 21 (12), 4377–4386.
Cetina-Heredia, P., Roughan, M., Van Sebille, E., Coleman, M., 2014. Long-term trends in the East Australian Current separation latitude and eddy driven transport. J. Geophys. Res.: Oceans 119 (7), 4351–4366.
Cetina-Heredia, P., Roughan, M., Liggins, G., Coleman, M.A., Jeffs, A., 2019a. mesoscale circulation determines broad spatiotemporal settlement patterns of lobster. Plus one 14 (2), e0211722.
Cetina-Heredia, P., Roughan, M., Van Sebille, E., Keating, S., Brassington, G.B., 2019b. Retention and leakage of water by mesoscale eddies in the East Australian Current system. J. Geophys. Res.: Oceans 124 (4), 2485–2500.
Chamberlain, M., Sun, C., Matear, R., Feng, M., Phipps, S., 2012. Downscaling the climate change for oceans around Australia. Geosci. Model Dev. 5 (5), 1177.
Chassignet, E.P., Marshall, D.P., 2008. Gulf Stream separation in numerical ocean models. Ocean Modeling in an Eddying Regime. Geophys. Monogr. 177, 39–61.
Chelton, D.B., Schlax, M.G., Samelson, R.M., 2011. Global observations of nonlinear mesoscale eddies. Prog. Oceanogr. 91, 167–216.
Chelton, D.B., Schlax, M.G., Samelson, R.M., de Szoeke, R.A., 2007. Global observations of large oceanic eddies. Geophys. Res. Lett. 34 (15), L15606.
Church, J.A., Craig, P.D., 1998. Australia's shelf seas: diversity and complexity coastal segment (30, ws).
Colin de Verdière, A., Ollitrault, M., 2016. A direct determination of the World Ocean barotropic circulation 46(1), 255–273.
Condie, S., Condie, R., 2016. Retention of plankton within ocean eddies. Glob. Ecol. Biogeogr. 25 (10), 1264–1277.
Condie, S., Mansbridge, J., Cahill, M., 2011. Contrasting local retention and cross-shore transports of the East Australian Current and the Leeuwin Current and their relative influences on the life histories of small pelagic fishes. Deep Sea Res. Part II: Top. Stud. Oceanogr. 58 (5), 606–615.
Cresswell, G., Zhou, C., Tildesley, P.C., Nilsson, C.S., 1996. SAR observations of internal wave wakes from sea mounts. Mar. Freshwater Res. 47, 489–495.
Cresswell, G., 1983. Physical evolution of Tasman Sea eddy. J. Mar. Freshwater Res. 34 (4), 495–513.
Cresswell, G.R., 1982. The coalescence of two East Australian Current warm-core eddies. Science 215 (4529), 161–164.
Cresswell, G.R., Legeckis, R., 1986. Eddies off southeastern Australia. Deep-Sea Res. 33 (11–12), 1527–1562.
Denham, R.N., Crook, F.G., 1976. The Tasman Front. New Zealand J. Mar. Freshwater Res. 10 (1), 15–30.
Ducet, N., Traon, P.-Y.L., Reverdin, G., 2000. Global high-resolution mapping of ocean circulation from TOPEX/POSEIDON and ERS-1 and-2. J. Geophys. Res. 105 (C8), 19477–19498.
Everett, J., Macdonald, H., Baird, M., Humphries, J., Roughan, M., Suthers, I., 2015. Cyclonic entrainment of preconditioned shelf waters into a frontal eddy. J. Geophys. Res.: Oceans 120 (2), 677–691.
Everett, J.D., Baird, M.E., Oke, P.R., Suthers, I.M., 2012. An avenue of eddies: quantifying the biophysical properties of mesoscale eddies in the Tasman Sea. Geophys. Res. Lett. 39 (L16608).
Feng, M., Zhang, X., Oke, P., Monselesan, D., Chamberlain, M., Matear, R., Schiller, A., 2016. Invigorating ocean boundary current systems around Australia during 1979–2014: as simulated in a near-global eddy-resolving ocean model. J. Geophys. Res.: Oceans 121 (5), 3395–3408.
Flierl, G.R., McGillicuddy, D.J., 2002. Mesoscale and submesoscale physical-biological interactions. In: Robinson, A.R., McCarthy, J.J., Rothschild, B. (Eds.), The Sea: Ideas and Observations on Progress in the Study of the Seas. Biological-Physical Interactions in the Sea, vol. 12. John Wiley and Sons, pp. 113–185.
Ganachaud, A., Cravatte, S., Melet, A., Schiller, A., Holbrook, N., Sloyan, B., Widlansky, M., Bowen, M., Verron, J., Wiles, P., et al., 2014. The Southwest Pacific Ocean circulation and climate experiment (SPICE). J. Geophys. Res.: Oceans 119 (11), 7660–7686.
Gibbs, M.T., Marchesiello, P., Middleton, J.H., 2000. Observations and simulations of a transient shelfbreak front over the narrow shelf at Sydney, southeastern Australia. Cont. Shelf Res. 20 (7), 763–784.

Godfrey, J.S., Cresswell, G.R., Golding, T.J., Pearce, A.F., 1980. The separation of the East Australian Current. J. Phys. Oceanogr. 10 (3), 430–440.
Godfrey, J.S., 1989. A sverdrup model of the depth-integrated flow for the world ocean allowing for island circulations. Geophys. Astrophys. Fluid Dyn. 45, 89–112.
Godfrey, J.S., Dunn, J.R., 2010. Depth-integrated steric height as a tool for detecting non-Sverdrup behavior in the global ocean. J. Mar. Res. 68 (3–4), 387–412.
Halligan, G.H., 1921. The ocean currents around Australia. J. Roy. Soc. New South Wales 55, 188–195.
Hamon, B., 1965. The East Australian Current, 1960–1964. Deep Sea Res. 12 (6), 899–921.
Hamon, B., 1980. The East Australian Current: review of work 1972–1977. In: Compte rendu de la réunion du groupe régional d'océanographie du Sud Ouest Pacifique proceedings of the regional workshop on the oceanography of the South West Pacific, pp. 73–77.
Harris, T., Legeckis, R., van Forest, D., 1978. Satellite infra-red images in the Agulhas Current System. Deep Sea Res. 25 (6), 543–548.
Hill, K.L., Rintoul, S.R., Coleman, R., Ridgway, K.R., 2008. Wind forced low frequency variability of the East Australia Current. Geophys. Res. Lett. 35 (8), L08602.
Hill, K.L., Rintoul, S.R., Ridgway, K.R., Oke, P.R., 2011. Decadal changes in the South Pacific western boundary current system revealed in observations and ocean state estimates. J. Geophys. Res. 116, C01009.
Hogg, N.G., Johns, W.E., 1995. Western boundary currents. Rev. Geophys. 33 (S2), 1311–1334.
Holbrook, N.J., Goodwin, I.D., McGregor, S., Molina, E., Power, S.B., 2011. ENSO to multi-decadal time scale changes in East Australian Current transports and fort denison sea level: Oceanic Rossby waves as the connecting mechanism. Deep Sea Res. 58 (5), 547–558.
Hu, D., Wu, L., Cai, W., Gupta, A.S., Ganachaud, A., Qiu, B., Gordon, A.L., Lin, X., Chen, Z., Hu, S., et al., 2015. Pacific western boundary currents and their roles in climate. Nature 522 (7556), 299–308.
Huyer, A., Smith, R.L., Stabeno, P.J., Church, J.A., White, N.J., 1988. Currents off southeastern Australia: results from the Australian coastal experiment. Mar. Freshwater Res. 39, 245–288.
Kawabe, M., 1995. Variations of current path, velocity, and volume transport of the Kuroshio in relation with the large meander. J. Phys. Oceanogr. 25, 3103–3117.
Kerry, C., Powell, B., Roughan, M., Oke, P., 2016. Development and evaluation of a high-resolution reanalysis of the East Australian Current region using the Regional Ocean Modelling System (ROMS 3.4) and Incremental Strong-Constraint 4-Dimensional Variational (IS4D-Var) data assimilation. Geosci. Model Dev. 9 (10), 3779.
Kerry, C., Roughan, M., Powell, B., 2018. Observation Impact in a Regional Reanalysis of the East Australian Current System. J. Geophys. Res.: Oceans 123 (10), 7511–7528.
Kessler, W.S., Cravatte, S., 2013. Mean circulation of the Coral Sea. J. Geophys. Res.: Oceans 118 (12), 6385–6410.
Koehl, A., Stammer, D., Cornuelle, B.D., 2007. Interannual to decadal changes in the ECCO global synthesis. J. Phys. Oceanogr. 37 (2), 313–337.
Le Traon, P., Dibarboure, G., Ducet, N., 2001. Use of a high-resolution model to analyze the mapping capabilities of multiple-altimeter missions. J. Atmosph. Oceanic Technol. 18, 1277–1288.
Macdonald, H., Roughan, M., Baird, M., Wilkin, J., 2013. A numerical modeling study of the East Australian Current encircling and overwashing a warm-core eddy. J. Geophys. Res.: Oceans 118 (1), 301–315.
Macdonald, H., Roughan, M., Baird, M., Wilkin, J., 2016. The formation of a cold-core eddy in the East Australian Current. Contin. Shelf Res. 114, 72–84.
Marchesiello, P., Middleton, J.H., 2000. Modeling the East Australian Current in the western Tasman Sea. J. Phys. Oceanogr. 30 (11), 2956–2971.
Martin, A.P., Richards, K.J., 2001. Mechanisms for vertical nutrient transport within a North Atlantic mesoscale eddy. Deep Sea Res. 48 (4), 757–773 The Biological Oceanography of the north-east Atlantic-the PRIME study.
Masumoto, Y., Sasaki, H., Kagimoto, T., Komori, N., Ishida, A., Sasai, Y., Miyama, T., Motoi, T., Mitsudera, H., Takahashi, K., Sakuma, H., Yamagata, T., 2004. A fifty-year eddy-resolving simulation of the world ocean: Preliminary outcomes of OFES (OGCM for the Earth Simulator). J. Earth Simul. 1, 35–56.
Mata, M.M., Tomczak, M., Wijffels, S.E., Church, J.A., 2000. East Australian Current volume transports at 30 degrees s: estimates from the World Ocean Circulation Experiment hydrographic sections PR11/P6 and the PCM3 current meter array. J. Geophys. Res. 105 (C12), 28509–28526.
Mata, M.M., Wijffels, S.E., Church, J.A., Tomczak, M., 2006. Eddy shedding and energy conversions in the East Australian Current. J. Geophys. Res. 111 (C9), C09034.
Matear, R., Chamberlain, M., Sun, C., Feng, M., 2013. Climate change projection of the Tasman Sea from an eddy-resolving ocean model. J. Geophys. Res.: Oceans 118 (6), 2961–2976.
McGillicuddy, D., Robinson, A.R., Siegel, D., Jannasch, H., Johnson, R., Dickeys, T., McNeil, J., Michaels, A., Knap, A., 1998. Influence of mesoscale eddies on new production in the Sargasso Sea. Nature 394 (6690), 263–266.
Mulhearn, P., Filloux, J., Lilley, F., Bindoff, N.L., Ferguson, I., 1988. Comparisons between surface, barotropic and abyssal flows during the passage of a warm-core ring. Austr. J. Mar. Freshwater Res. 39 (6), 697–707.
Mullaney, T., Miskiewicz, A., Baird, M., Burns, P., Suthers, I., 2011. Entrainment of larval fish assemblages from the inner shelf into the East Australian Current and into the western Tasman Front. Fisher. Oceanogr. 20 (5), 434–447.
Nardelli, B.B., Oct 2013. Vortex waves and vertical motion in a mesoscale cyclonic eddy. J. Geophys. Res.: Oceans 118 (10), 5609–5624.
Nilsson, C., Cresswell, G., 1980. The formation and evolution of East Australian Current warm-core eddies. Prog. Oceanogr. 9 (3), 133–183.
Nof, D., Dewar, W., 1994. Alignment of lenses: laboratory and numerical experiments. Deep Sea Res. 41 (8), 1207–1229.
Oke, P.R., Brassington, G.B., Griffin, D.A., Schiller, A., 2008. The Bluelink Ocean Data Assimilation System (BODAS). Ocean Model. 21 (1–2), 46–70.
Oke, P.R., England, M.H., 2004. Oceanic response to changes in the latitude of the southern hemisphere subpolar westerly winds. J. Clim. 17 (5), 1040–1054.
Oke, P.R., Griffin, D.A., 2011. The cold-core eddy and strong upwelling off the coast of New South Wales in early 2007. Deep Sea Res. 58 (5), 574–591.
Oke, P.R., Griffin, D.A., Schiller, A., Matear, R.J., Fiedler, R., Mansbridge, J.V., Lenton, A., Cahill, M., Chamberlain, M.A., Ridgway, K., 2013. Evaluation of a near-global eddy-resolving ocean model. Geosci. Model Dev. 6, 591–615.
Oke, P.R., Middleton, J.H., 2001. Nutrient enrichment off Port Stephens: the role of the East Australian current. Contin. Shelf Res. 21 (6–7), 587–606.
Oke, P.R., Sakov, P., Cahill, M.L., Dunn, J.R., Fiedler, R., Griffin, D.A., Mansbridge, J.V., Ridgway, K.R., Schiller, A., 2013. Towards a dynamically balanced eddy-resolving ocean reanalysis: BRAN3. Ocean Model. 67, 52–70.
Oke, P.R., Pilo, G.S., Ridgway, K., Kiss, A., Rykova, T., 2019. A search for the Tasman Front. J. Marine Systems 199, 103217.
Oliver, E., Holbrook, N., 2014. Extending our understanding of South Pacific gyre "spin-up": modeling the East Australian Current in a future climate. J. Geophys. Res.: Oceans 119 (5), 2788–2805.
Oliver, R.J., Benthuysen, J.A., Bindoff, N.L., Hobday, A.J., Holbrook, N.J., Mundy, C.N., Perkins-Kirkpatrick, S.E., 2017. The unprecedented 2015/16 Tasman Sea marine heatwave. Nat. Commun. 8 16101 EP – 288.
Olson, D.B., Podesta, G.P., Evans, R.H., Brown, O.T., 1988. Temporal variations in the separatyion of Brazil and Malvinas Currents. Deep Sea Res. 12, 1971–1990.
Pilo, G.S., Mata, M.M., Azevedo, J.L.L., 2015a. Eddy surface properties and propagation at southern hemisphere western boundary current systems. Ocean Sci. 11 (4), 629–641.
Pilo, G.S., Oke, P.R., Coleman, R., Rykova, T., Ridgway, K., 2018. Patterns of vertical velocity induced by eddy distortion in an ocean model. J. Geophys. Res.: Oceans 123 (3), 2274–2292.
Pilo, G.S., Oke, P.R., Rykova, T., Coleman, R., Ridgway, K., 2015b. Do East Australian Current anticyclonic eddies leave the Tasman Sea? J. Geophys. Res.: Oceans 120 (12), 8099–8114.
Qiu, B., Chen, S., 2004. Seasonal modulations in the eddy field of the South Pacific Ocean. J. Phys. Oceanogr. 34 (7), 1515–1527.
Reid, J.L., 1986. On the total geostrophic circulation of the South Pacific Ocean: flow patterns, tracers and transports. Prog. Oceanogr. 16 (1), 1–61.
Richardson, P.L., Knauss, J.A., 1971. Gulf stream and western boundary undercurrent observations at Cape Hatteras. Deep Sea Res. Oceanogr. Abstr. 18 (11), 1089–1109.
Ridgway, K., 2007. Long-term trend and decadal variability of the southward penetration of the East Australian Current. Geophys. Res. Lett. 34 (13).
Ridgway, K., Coleman, R., Bailey, R., Sutton, P., 2008. Decadal variability of East Australian Current transport inferred from repeated high-density XBT transects, a CTD survey and satellite altimetry. J. Geophys. Res.: Oceans (1978–2012) 113 (C8).
Ridgway, K., Dunn, J., 2007. Observational evidence for a southern hemisphere oceanic supergyre. Geophys. Res. Lett. 34 (13).
Ridgway, K., Godfrey, J., 1994. Mass and heat budgets in the East Australian Current: a direct approach. J. Geophys. Res.: Oceans (1978–2012) 99 (C2), 3231–3248.
Ridgway, K.R., Dunn, J.R., 2003. Mesoscale structure of the mean East Australian Current System and its relationship with topography.
Ridgway, K.R., Godfrey, J.S., 1997. Seasonal cycle of the East Australian Current. J. Geophys. Res. 102 (C10), 22921–22936.
Risien, C.M., Chelton, D.B., 2008. A global climatology of surface wind and wind stress fields from eight years of QuikSCAT scatterometer data. J. Phys. Oceanogr. 38 (11), 2379–2413.
Rochford, D.J., 1983. Origins of water within warm-core eddies of the western Tasman Sea. Mar. Freshwater Res. 34, 525–534.
Roemmich, D., Gilson, J., 2001. Eddy transport of heat and thermocline waters in the North Pacific: a key to interannual/decadal climate variability? J. Phys. Oceanogr. 31 (3), 675–687.
Roemmich, D., Gilson, J., Davis, R., Sutton, P., Wijffels, S., Riser, S., 2007. Decadal spinup of the South Pacific subtropical gyre. J. Phys. Oceanogr. 37 (2), 162–173.
Roughan, M., Keating, S., Schaeffer, A., Cetina Heredia, P., Rocha, C., Griffin, D., Robertson, R., Suthers, I., 2017. A tale of two eddies: the biophysical characteristics of two contrasting cyclonic eddies in the East Australian Current System. J. Geophys. Res.: Oceans 122 (3), 2494–2518.
Roughan, M., Middleton, J.H., 2002. A comparison of observed upwelling mechanisms off the east coast of Australia. Contin. Shelf Res. 22 (17), 2551–2572.
Roughan, M., Oke, P.R., Middleton, J.H., 2003. A modeling study of the climatological current field and the trajectories of upwelled particles in the East Australian Current. J. Phys. Oceanogr. 33 (12), 2551–2564.
Rykova, T., Oke, P.R., 2015. Recent freshening of the East Australian Current and its eddies. Geophys. Res. Lett. 42 (21), 9369–9378.
Rykova, T., Oke, P.R., Griffin, D.A., 2017. A comparison of the structure, properties, and water mass composition of quasi-isotropic eddies in western boundary currents in an eddy-resolving ocean model. Ocean Model. 114, 1–13.
Schaeffer, A., Gramoulle, A., Roughan, M., Mantovanelli, A., 2017. Characterizing frontal eddies along the East Australian Current from HF radar observations. J. Geophys. Res.: Oceans 122 (5), 3964–3980.
Schaeffer, A., Roughan, M., 2015. Influence of a western boundary current on shelf dynamics and upwelling from repeat glider deployments. Geophys. Res. Lett. 42 (1), 121–128.
Scharffenberg, M.G., Stammer, D., 2010. Seasonal variations of the large-scale geostrophic flow field and eddy kinetic energy inferred from the TOPEX/Poseidon and Jason-1 tandem mission data. J. Geophys. Res. 115, C02008.
Schiller, A., Oke, P.R., Brassington, G.B., Entel, M., Fiedler, R., Griffin, D.A., Mansbridge,

J.V., 2008. Eddy-resolving ocean circulation in the Asian-Australian region inferred from an ocean reanalysis effort. Prog. Oceanogr. 76 (3), 334–365.
Schoonover, J., Dewar, W.K., Wienders, N., Deremble, B., 2017. Local sensitivities of the Gulf Stream Separation. J. Phys. Oceanogr. 47, 353–373.
Sloyan, B.M., O'Kane, T.J., 2015. Drivers of decadal variability in the Tasman Sea. J. Geophys. Res.: Oceans 120 (5), 3193–3210.
Sloyan, B.M., Ridgway, K.R., Cowley, R., 2016. The East Australian Current and property transport at 27S from 2012 to 2013. J. Phys. Oceanogr. 46 (3), 993–1008.
Speich, S., Blanke, B., de Vries, P., Drijfout, S., Doos, K., Ganachaud, A., Marsh, R., 2002. Tasman leakage: a new route in the global ocean conveyer belt. Geophys. Res. Lett. 29 (10). https://doi.org/10.1029/2001GL014586.
Stanton, B.R., 1979. The Tasman Front. New Zealand J. Mar. Freshwater Res. 13 (2), 201–214.
Stanton, B.R., 1981. An oceanographic survey of the Tasman Front. New Zealand J. Mar. Freshwater Res. 15 (3), 289–297.
Stramma, L., Peterson, R.G., Tomczak, M., 1995. The South Pacific current. J. Phys. Oceanogr. 25, 77–91.
Sun, C., Feng, M., Matear, R., Chamberlain, M., Craig, P., Ridgway, K., Schiller, A., 2012. Marine downscaling of a future climate scenario for Australian boundary currents. J. Clim. 25, 2947–2962.
Suthers, I.M., Everett, J.D., Roughan, M., Young, J.W., Oke, P.R., Condie, S.A., Hartog, J.R., Hobday, A.J., Thompson, P.A., Ridgway, K., Baird, M.E., Hassler, C.S., Brassington, G.B., Byrne, M., Holbrook, N.J., Malcolm, H.A., 2011. The strengthening East Australian Current, its eddies and biological effects – an introduction and overview. Deep-Sea Res. 58 (5), 538–546.
Sutton, P.J., Bowen, M., 2014. Flows in the Tasman front south of Norfolk Island. J. Geophys. Res.: Oceans 119 (5), 3041–3053.
Tilburg, C.E., Hurlburt, H.E., O'Brien, J.J., Shriver, J.F., 2001. The dynamics of the East Australian Current system: the Tasman Front, the East Auckland Current, and the East Cape Current. J. Phys. Oceanogr. 31 (10), 2917–2943.
Tranter, D., Leech, G., Vaudrey, D., 1982. Biological significance of surface flooding in warm-core ocean eddies. Nature 297, 572–574.
van Sebille, E., Biastoch, A., van Leeuwen, P.J., de Ruijter, W.P.M., 2009. A weaker Agulhas Current leads to more Agulhas leakage. Geophys. Res. Lett. 36 (3), l03601.
van Sebille, E., England, M.H., Zika, J.D., Sloyan, B.M., 2012. Tasman leakage in a fine-resolution ocean model. Geophys. Res. Lett. 39 (6).
Warren, B.A., Voorhis, A.D., 1970. Velocity measurements in the deep Western Pacific Current of the South Pacific. Nature 229, 849–850.
Wijeratne, S., Pattiaratchi, C., Proctor, R., 2018. Estimates of surface and subsurface boundary current transport around Australia. J. Geophys. Res.: Oceans 123.
Wilkin, J.L., Zhang, W., 2007. Modes of mesoscale sea surface height and temperature variability in the East Australian Current. J. Geophys. Res. 112 (C1), C01013.
Wood, J., Schaeffer, A., Roughan, M., Tate, P., 2016. Seasonal variability in the continental shelf waters off southeastern Australia: fact or fiction? Contin. Shelf Res. 112, 92–103.
Wu, L., Cai, W., Zhang, L., Nakamura, H., Timmermann, A., Joyce, T., McPhaden, M.J., Alexander, M., Qui, B., Visbeck, M., Chang, P., Giese, B., 2012. Enhanced warming over the global subtropical western boundary currents. Nat. Clim. Change 2, 161–166.
Wyrtki, K., 1962. Geopotential topographies and associated circulation in the western South Pacific Ocean. Mar. Freshwater Res. 13 (2), 89–105.
Ypma, S., van Sebille, E., Kiss, A., Spence, P., 2016. The separation of the east australian current: a lagrangian approach to potential vorticity and upstream control. J. Geophys. Res.: Oceans 121 (1), 758–774.
Zilberman, N., Roemmich, D., Gille, S., Gilson, J., 2018. Estimating the velocity and transport of western boundary current systems: a case study of the East Australian Current near Brisbane. J. Atmosph. Oceanic Technol. (2018).
Zilberman, N.V., Roemmich, D.H., Gille, S.T., 2014. Meridional volume transport in the South Pacific: mean and SAM-related variability. J. Geophys. Res.: Oceans 119 (4), 2658–2678.